Murine hypoglossal motor neuron topographic map development

A thesis submitted to McGill University in partial fulfillment of the requirements for the degree of Master of Science in Cell Biology

Jae Woong Wang

Department of Anatomy and Cell Biology

McGill University

Montreal, Quebec

April 2016

Dedication

This thesis is dedicated to further our grasp of knowledge of motor neuron biology, hoping to benefit patients suffering from motor neuron diseases.

Acknowledgement

I whole-heartedly thank every current and past members of the Stifani Lab for their priceless emotional support, impeccable technical guidance, brainstorming aid, and practically everything. Listed in alphabetic order: Dr. Adele Salin-Cantegrel, Dr. Federica Verginelli, Dr. Federica Trombin, Karen Fung, Katherine Li, Dr. Laurent Methot, Lawrie Shahbazian, Marielle Beaulieu, Rita Lo, Rola Dali, Sara Benchekroun, Dr. Valerio Piscopo, Dr. Vincent Soubannier, Dr. Xin Chen, and Dr. YeMan Tang

Also great amount of thanks to neighboring Cloutier Lab for allowing the use of their microscope, most-productive hallway chat, and occasional free yummies. Listed in alphabetical order: Alex Brignall, Candice Wiedman, Chris Baim, Emily Dumontier, Dr. Jean-Francois Cloutier, Dr. Joseph Lam, Katrine Iversen, and Reesha Raja.

I would also like to extend my thanks to other members of the Montreal Neurological Institute that I will hold very dear.

I also recognize and thank members of my committee for their precious feedbacks. Listed in alphabetical order: Dr. Artur Kania, Dr. Jean-Francois Cloutier, and Dr. Nathalie Vane-Lamarche (my graduate mentor).

With much respect and many thanks, I would like to recognize my supervisor Dr. Stefano Stifani whom I have learned so much from.

We thank Dr. Artur Kania for the $Hb9^{Cre}$ mice, Dr. Silva Arber for the Tau^{Runx1} mice, Dr. Jeremy Dasen for anti-SCIP antibodies, and Dr. Jean-Francois Cloutier for microscopy support.

We also thank Mireille Bouchard-Levasseur and Stephanie Perrino for invaluable help with animal care.

I thank Dr. Vincent Soubannier for help in composing the French translation of the abstract.

Thanks to mum and dad for the unconditional support that I received.

Forever in debt to all individuals above.

Preface & Contributions

I declare that I composed this Thesis entitled “Murine hypoglossal motor neuron topographic map development” edited by my supervisor Dr. Stefano Stifani. Moreover, I performed the work listed below, including design and data collection:

- Schematic drawing of summary of results obtained by Dr. Xin Chen (Figure 4).
- Co-expression study of PV and CGRP in the developing 12N *Runx1*^{LacZ} mice (Figure 5).
- Expression analysis of Calbindin and SCIP in the developing 12N (Figures 6-9)
- Effects of ectopic Runx1 expression along the three 12N axes (Figures 11-14, except Figure 12c)
- Schematic summary of expression study and possible role of Runx1 in 12N (Figures 10,15)

The following individuals contributed to work discussed in this Thesis:

- Dr. Stefano Stifani for advice in experimental design and analysis and for writing the publication (Chen et al., 2015)
- Dr. Xin Chen initiated the project and carried out the following analyses:

  -Characterization of *Runx1* expression in *Runx1*^{LacZ} mice (Chen et al., 2015).

  -Retrograde labelling studies in *Runx1*^{LacZ} mice (Chen et al., 2015).

  -Characterization of FoxP1, PV, CGRP, and calretinin expression pattern in *Runx1*^{LacZ} mice (Chen et al., 2015).

  -Analysis of changes to dorsomedial group of 12N MNs upon ectopic expression of Runx1 in Tau^{Runx1}Hb9^{Cre} mice (Chen et al., 2015).

- Ms. Rola Dali carried out the *in silico* analysis of putative Runx1 binding sites on various promotor regions (Chen et al., 2015).
- Dr. Adele Salin-Cantegrel carried out the analysis regarding changes in CGRP expression between Tau^{Runx1}Hb9^{Cre} and Tau^{Runx1} (Chen et al., 2015).

Abstract

Motor neurons (MNs) are essential neuronal cells that play unique roles in functional motor circuits. During development, somatic MNs topographically organize into distinct subtypes that innervate specific muscle targets. The acquisition of topologically defined MN groupings is an essential process during the development of the mouse hypoglossal nucleus, a structure located in the caudal brainstem. Hypoglossal MNs innervate tongue muscles controlling vital functions such as mastication, swallowing, and respiration. These MNs attract considerable research interest due to their vulnerability to degeneration in MN diseases like Amyotropic Lateral Sclerosis, where loss of hypoglossal MNs is a contributing factor to patient morbidity and mortality by impairing feeding and respiratory functions. The establishment of precise MN maps within the hypoglossal nucleus is essential for the formation of functional motor circuits controlled by hypoglossal MNs innervating tongue muscles. However, little is known about the mechanisms underlying the establishment of hypoglossal MN somatotopic maps. To address this lack of information, work presented in this thesis sought to understand the molecular mechanisms controlling the establishment of specific hypoglossal MN identities and topologies using a combination of in vivo expression studies and genetic perturbation analyses. These investigations provided evidence that the expression of three transcription factors, termed Runx1, FoxP1, and SCIP, defines anatomical subdivisions of the hypoglossal nucleus containing MNs with unique topological, neurotransmitter, and calcium buffering phenotypes. More specifically, Runx1 and SCIP are expressed in a group of ventromedial hypoglossal MNs that innervate muscles involved in tongue protrusion. In contrast, FoxP1 is expressed in a separate group of hypoglossal MNs dorsal to the Runx1-expressing MNs and hypothesized to mediate tongue retraction. Additionally, results of in vivo gain-of-function studies provided evidence that Runx1 is important for the establishment of MN topology in the hypoglossal nucleus, at least in part, by restricting the expression of FoxP1 and SCIP. These combined results suggest that the distinct expression pattern of transcription factors Runx1, FoxP1, and SCIP contributes to the development of vital motor circuits controlling tongue protrusion and retraction in part through the establishment of the hypoglossal MN topographic map.

Résumé

Les motoneurones (MNs) sont des cellules neuronales essentielles qui jouent des rôles uniques dans les circuits moteurs fonctionnels. Au cours du développement, les MNs somatiques s'organisent topographiquement en sous-types distincts lesquels innervent des cibles musculaires spécifiques. L'acquisition de groupements de MN topologiquement définis est un processus essentiel au cours du développement du noyau hypoglosse de la souris, une structure située dans le tronc cérébral caudal. Les MNs hypoglossaux innervent les muscles de la langue, contrôlant ainsi des fonctions vitales telles que la mastication, la déglutition et la respiration. Ces MNs suscitent un intérêt considérable en recherche en raison de leur vulnérabilité à la dégénérescence dans des maladies neurodégénératives comme la Sclérose Latérale Amyotrophique (SLA), où la perte de MNs hypoglossaux est un facteur contribuant à la morbidité et la mortalité des patients en altérant l'alimentation et les fonctions respiratoires. La mise en place de cartes précises de MN dans le noyau hypoglosse est essentielle pour la formation de circuits moteurs fonctionnels commandés par ces MNs hypoglossaux qui innervent les muscles de la langue. Cependant, on sait peu sur les mécanismes sous-jacents de la création des cartes somatotopiques de MN hypoglossaux. Pour remédier à ce manque d'information, le travail présenté dans cette thèse a cherché à comprendre les mécanismes moléculaires contrôlant la mise en place des identités et des topologies spécifiques des MN hypoglossaux en utilisant une combinaison d'études d'expression *in vivo* et d'analyse par perturbation génétique. Ces recherches ont fourni la démonstration que l'expression de trois facteurs de transcription; appelés Runx1, FOXP1 et SCIP; définit les subdivisions anatomiques du noyau hypoglosse, lesquelles subdivisions possèdent des MNs avec des phénotypes uniques topologiques, de neurotransmission, et de pouvoir tampon du calcium. Plus précisément, Runx1 et SCIP sont exprimés dans un groupe de MNs hypoglossaux ventro-médians qui innervent les muscles impliqués dans protrusion de la langue. En revanche, FOXP1 est exprimé dans un groupe distinct de MNs hypoglossaux, groupe situé en position dorsale par rapport aux MNs exprimant Runx1, et ce groupe de MNs exprimant FOXP1 contrôleraient la rétraction de la langue. En outre, les résultats d'études de gain de fonction *in vivo* fournissent des preuves que Runx1 est important

pour l'établissement de la topologie des MNs dans le noyau hypoglosse, au moins en partie, en limitant l'expression de FOXP1 et SCIP. Ces résultats combinés suggèrent que la mosaïque d'expression bien circonscrite de facteurs de transcription tels que Runx1, FOXP1 et SCIP contribue au développement des circuits moteurs vitaux qui contrôlent la protrusion et la rétraction de la langue, en partie grâce à la mise en place de la carte topographique de l’hypoglosse.

Table of Contents

Chapter 1: Preamble

One of the fundamental pillars constituting the definition of life is the ability of an organism to respond to various environmental stimuli. Historically, observation of life-defining responses began by looking for signs of motion. In the Kingdom of Animalia, movement is often achieved through the contraction of muscle fibers that respond to input from the nervous system. In vertebrates, the nervous system is composed of inter-connected networks of neurons that form circuits to receive information from the environment, integrate, and respond by producing appropriate outputs. Some of the key neural behaviors in sustaining life of a vertebrate include feeding and respiration, activities that are in part coordinated by a unique muscular organ called the tongue. Throughout evolution, from fish to mammals, the tongue has evolved to carry out many other non-vital motor functions such as coughing, licking, and speaking to name a few. These vital and non-vital movements coordinated by the tongue are made possible by specific innervation of the different muscles of the tongue by motor neurons of the hypoglossal nucleus. Regardless of the species-specific uses of the tongue, one of the fundamental mode of movement underlying most tongue neural circuit is the final output of either protrusion or retraction of the tongue. Central to such evolutionarily-conserved neural circuitry lies an important question to be asked. How is the ‘hypoglossal circuit’ established to regulate movements of the tongue?

Chapter 2: Introduction

Throughout evolution, species have constantly evolved to better adapt to their changing environment. This adaptation meant in part improving the ability of the nervous system to respond to the environment. Subsequently, the nervous system had to constantly evolve methods to perceive the given stimulus, interpret the information, and finally generate a response that best suits the situation. Such responses are frequently observed in the form of movement, which is generated by contraction of muscle fibers as a result of neural stimulation. The network of inter-connecting neurons that coordinate the appropriate neural output for movement is called a motor circuit.

A motor circuit can be described by referring to studies of the spinal cord reflex circuitry. There are three main neuron types that are involved in a basic sensory-motor circuit. First, sensory neurons of the dorsal root ganglia (DRG) receive various stimuli from the external and internal environment. These sensory neurons either synapse directly onto motor neurons (MNs) or relay signal to a second type of neurons called interneurons. Interneurons process information and eventually convey information towards MNs. MNs that receive input stimulate their respective muscle targets to generate muscle contraction, eventually leading to movement (Eccles et al., 1957; Hultborn, 2006; Stifani, 2014). Although simply described herein, the complexity of the system is vast considering the large quantity of information that is received from various sources including various sensory organs and the muscle itself. In addition, this multitude of information may involve communication with other circuits of the brain and must be processed in real-time to generate a timely response.

When considering that the human body contains at least 300 bilateral pairs of muscles, we realize the complexity in the number of circuits besides the complexity of each individual circuit (Kanning et al., 2010). In this regard, MNs occupy a critical function in each circuit as they are the neural component of motor circuits that directly synapse onto the final peripheral targets. This implies that as diverse as the number of circuits and the number of muscles are, the diversity of MNs must correspond to such numbers. Additionally, by either lack or excess of diversity of MNs, signals from the central nervous system (CNS) cannot be efficiently relayed to the final peripheral target

as MNs serve as the final component in which multiple inputs converge upon. Taken together, MNs play a critical role in the function of each motor circuit and the diversity of MNs is also critical for generation of multiple circuits.

Given their crucial role, perturbations of the functions of MNs usually lead to critical outcomes. An example of a disease that affects MNs is Amyotrophic Lateral Sclerosis (ALS). MNs of patients affected by ALS progressively degenerate and patients eventually lose control over muscles important for sustaining life. One of the defining pathology of ALS is that certain MNs are more susceptible to degeneration than others (Gordon et al., 2003; Sharma et al., 2011). By studying the properties of different groups of MNs that are more or less vulnerable to degeneration, we may gain further insights into ALS pathology and identify targets for therapeutic manipulations (Brockington et al., 2014). In this regard, studies of the development of specific groups of MNs may provide previously unidentified molecular pathways important for resistance and survival of ALS-vulnerable MNs.

With the advent of technologies in reprogramming embryonic stem cells (ESCs) and induced-pluripotent stem cells (iPSCs), it has become possible to derive MNs in vitro with the aim of modeling MN diseases and possibly develop in vitro drug screening assays (Han et al., 2011; Grskovic et al., 2011; Du et al., 2015; Sances et al., 2016). This not only involves directed generation of MNs, but also generation of specific types of MNs that are more relevant for ALS pathology as not all MNs are equally sensitive to degeneration or vital for survival. To improve our understanding of how to specifically direct stem cells to generate specific types of MNs, it is necessary to study the natural generation of MN diversity. By identifying molecular pathways involved in MN development, we may expand our understanding of general developmental processes underlying generation and maintenance of MN diversity, and further bolster our approach to screening effective drug treatments for ALS in vitro.

One of the group of MNs that are highly susceptible to ALS degeneration are the MNs of the hypoglossal nucleus (12N). During development, MNs of the 12N (i.e., hypoglossal MNs) extend axons to innervate various muscles of the tongue. Consequently, MNs of the 12N play important role in the coordination of vital processes

performed by the tongue such as chewing, swallowing and breathing (Lowe 1980, 1984; Sawczuk & Mosier, 2001; Fregosi, 2011). One interesting feature of 12N MNs is that they are organized into a somatotopic map, meaning that subgroups of MNs, whose axons converge to innervate a specific muscle, are found in specific developmentally programmed coordinates, or topology. Establishment of a somatotopic map is an evolutionarily conserved mechanism for organisms to efficiently wire the motor circuits for functional outputs (Bikeles, 1905; Romanes, 1951; Ramón y Cajal 1989). The genetic programs regulating somatotopic development of spinal cord MNs have been the subject of numerous studies, yet there is a lack of knowledge regarding development of the 12N somatotopic map.

To address this lack of information, work presented in this thesis sought to understand the molecular mechanisms controlling the establishment of specific 12N MN identities and topologies. In order to provide a brief introduction to MN development, discussions of the relevant literature regarding generation and diversification of MNs will be provided hereafter through examples taken from studies of spinal cord and brainstem MNs.

[2.1] Diversity of motor neurons

Vertebrate MNs can be classified into two main categories, named upper motor neurons and lower motor neurons.

[2.1.1] Upper motor neurons

Upper MNs are located in select areas of the brainstem and cortex, including cortical areas of the frontal lobe. Upper MNs carry out different functions that involve forming glutamatergic synapse onto lower MNs or other upper MNs that eventually relay signals to lower MNs. In general, upper MNs are thought to indirectly influence the generation of movements by directly affecting and modulating the local motor circuits in the brainstem and spinal cord (Purves and Williams, 2004; Stifani, 2014).

[2.1.2] Lower motor neurons

Lower MNs are located in specific nuclei within the brainstem and the ventral horn of the spinal cord. As mentioned above, lower MNs receives inputs from upper MNs, sensory neurons, and interneurons. Unlike upper MNs, lower MNs form cholinergic synapses onto muscle targets to form neuromuscular junctions. Specifically, MNs of the brainstem are organized into small groups called cranial nuclei and innervate muscles of the head and face, such as tongue, jaw, and neck muscles. Spinal cord MNs (SpMNs) innervate other skeletal muscles of the body. Depending on muscle targets, lower MNs may be further classified into three categories: branchial, visceral, and somatic MNs.

[2.1.2.1] Branchial motor neurons

Branchial MNs are located in the brainstem and innervate muscles derived from the branchial arches. These branchial MNs, also named branchiomotor (BM) neurons, are found in specific cranial nuclei including the trigeminal (5N), facial (7N), glossopharyngeal (9N), vagus (10N), and accessory (11N) nuclei (Gilland and Baker, 1993; Guthrie, 2007, Stifani 2014).

[2.1.2.2] Visceral motor neurons

Visceral MNs innervate and control involuntary functions of the smooth muscles and glands. As part of the autonomic nervous system, visceral MNs may be further divided into sympathetic and parasympathetic MNs by their functions. In the brainstem, visceral MNs are found in cranial nuclei including the superior salivary (7N) and dorsal motor nucleus of vagus (10N) nuclei (Gilland and Baker, 1993; Guthrie, 2007, Stifani 2014).

[2.1.2.3] Somatic motor neurons

Somatic MNs are located in the brainstem and spinal cord and innervate muscles derived from somites. These are skeletal muscles that coordinate movements such as breathing and walking. In the brainstem, there are four somatic MNs located in 4 cranial nuclei including oculomotor (3N), trochlear (4N), abducens (6N), and 12N (hypoglossal) nuclei (Guthrie, 2007). One of the defining characteristics of somatic MNs is the ventral exit trajectory of axons with the exception of 4N. Somatic MNs may be further subdivided into three groups: alpha, beta, and gamma depending on the type of muscle fiber innervated (Kanning et al., 2010, Stifani, 2014). From this point onwards, our discussion will be focused to somatic MNs as this will provide relevant information regarding 12N.

[2.2] Generation of somatic motor neurons

Decades of studies of SpMNs have characterized the development of somatic MNs. This chapter is organized to discuss key concepts behind the generation of somatic MNs. To exemplify our understanding, studies in SpMNs will be discussed as well as MNs of the hindbrain, including 12N MNs.

[2.2.1] Rostro-caudal specification of the neural tube

Along the rostro-caudal axis, the neural tube is specified into different parts, such as the forebrain, midbrain, hindbrain, and spinal cord, during development. It is thought that gradients of specific signaling molecules direct the differentiation of neuronal types. For instance, one of the molecules contributing to caudalization of the spinal cord is retinoid acid (RA). Produced through the activity of retinaldehyde dehydrogenase 2 (RALDH-2), RA was shown to be necessary for initial segmentation of hindbrain and spinal cord from more rostral structures such as forebrain and midbrain (Maden, 2007). In addition to RA, other diffusible proteins such as fibroblast growth factor (FGF) were shown to pattern the neural tube by creating a gradient (rostral-low and caudal-high) along the rostro-caudal axis (Liu et al., 2001). During the development of midbrain-hindbrain boundary, FGF8 is considered a 'master' initiator involved in regulation of important genes such as *Lrrn1,* while FGF8 signaling is tightly regulated at post-transcriptional level by miR9 (Leucht et al., 2008; Tossell et al., 2011; Dworkin & Jane, 2013). In Zebrafish, miR9 is expressed in regions around the midbrain-hindbrain boundary and targets several components of the Fgf pathway such as *fgf*8, *fgfr*1, and *canopy*1 for degradation, delimiting the midbrain-hindbrain organizer zone and allowing Fgf8 signaling to inhibit neurogenesis in midbrain-hindbrain boundary (Leucht et al., 2008). In mammals, miR9 has been shown to negatively regulate hes-family member *hairy*1 (*her*5 in zebrafish), possibly by causing RNA instability, which is speculated to be important for regulating oscillatory dynamics of hes-family member levels (Bonev et al., 2011).

Influenced by concentration of diffusible molecules such as FGFs and RA, genes of the *Hox* family containing Antennapedia-class homeobox sequence are transcribed in a region-specific pattern in a dose-dependent manner. *Hox* genes are organized in clusters on four separate chromosomes (HoxA, HoxB, HoxC, HoxD) each of which harbours 13 paralogue groups (Hox1-13) (McGinnis & Krumlauf, 1992). The responsiveness of each *Hox* gene to RA and FGFs is determined by the position of each gene within the cluster. For example, *Hox* genes closer to the 5' end of the gene cluster are transcribed in response to high FGF concentrations, thus expressed more caudally. Conversely, *Hox* genes located closer to 3' end of the gene cluster are activated in response to low FGF concentrations and expressed more rostrally (Liu et al., 2001). Moreover, Hox proteins cross-repress each other to establish non-overlapping domains throughout the hindbrain and spinal cord. In addition to segmenting the neural tube into different components, Hox proteins play important roles in diversifying generic immature MNs into specific subtypes (Philippidou & Dasen, 2013; Francius & Clotman, 2014).

[2.2.2] Dorso-ventral patterning of the spinal cord

Along the dorso-ventral axis, the ventral spinal cord is patterned into 5 different progenitor domains, described as p0, p1, p2, pMN, and p3, that give rise to various interneuron subtypes and MNs (Figure 1A). Dorso-ventral patterning is initially dependent on gradients of inductive signaling molecules, otherwise known as morphogens, secreted from ventral and dorsal regions of the spinal cord. For instance, in the ventral spinal cord, sonic hedgehog (Shh) is released from the notochord and floor plate, creating a gradient of ventral-high and dorsal-low Shh concentration (Yamada et al., 1991, 1993). In the dorsal spinal cord, members of the wingless-type MMTC integration site family (WNT) and members of the bone morphogenic protein family (BMPs) are secreted to form ventral-low and dorsal-high gradients (Alvarez-Medina et al., 2008, Mehler et al., 1997). Depending on the specific concentration of dorsal and ventral morphogens received, progenitor cells in the ventral half of the neural tube eventually express homeodomain (HD) and basic helix-loop-helix (bHLH)

transcription factors that can be divided in two categories: Class I and Class II proteins (Alaynick et al., 2011). Class II proteins such as NK2 homeobox 2 and 9 (Nkx2.2/2.9), NK6 homeobox 1 and 2 (Nkx6.1/6.2), and oligodendrocyte transcription factor 2 (Olig2) are upregulated in progenitor cells found ventrally. Conversely, Class I proteins such as paired box 3/6/7 (Pax3/6/7), developing brain homeobox 1 and 2 (Dbx1/2) and Iroquois related homeobox 3 (Irx3) are upregulated in progenitor cells found dorsally (Briscoe et al., 2000; Jessell, 2000; Shirasaki and Pfaff, 2002; Alaynick et al., 2011). These class I and class II proteins play important roles in consolidating progenitor identity but also in delineating the boundaries between adjacent progenitor domains by cross-repressive activity. For example, possible cross-repression between Pax6 and Nkx2.2 were originally suggested to set the boundary between p3 and pMN, with the pMN domain giving rise to MNs (Ericson et al., 1997; Briscoe et al., 1999, 2000). A more recent study has suggested that a zinc-finger protein, Sp8, plays supplementary roles to Pax6 in delineating the p3/pMN boundary through cross-repressive interactions with Nkx2.2 (Li et al., 2014). Dorsal to the pMN domain, cross-repression between Irx3 and Olig2 allows p2 and pMN domains to be mutually exclusive (Novich et al., 2001). Eventually, the 5 different progenitor domains are specified and these progenitors rapidly proliferate and eventually differentiate to give rise to MNs and V0, V1, V2, and V3 interneurons (Figure 1A).

[2.2.3] Dorso-ventral patterning of the brainstem

Brainstem MNs arise from two different progenitor domains, in contrast to SpMNs which arise from one progenitor domain, pMN. In the hindbrain, the progenitor domain adjacent to the floor plate (i.e., p3) give rise to branchial and visceral MNs, whereas the pMN domain dorsal to the p3 domain gives rises to somatic MNs (Figure 1B). The dorso-ventral patterning of the brainstem is also thought to occur using similar molecular pathways as the spinal cord. For instance, Shh-mediated signaling has also been shown to pattern the brainstem as loss of Shh expression leads to loss of brainstem MNs (Litingtung and Chiang, 2000). Additionally, many of the class I and class II transcription factors discussed above have been shown to be important for

regulating specification of progenitor domains. In the p3 domain, Nkx 2.2 and 2.9 act by repressing expression of interneuron-related genes to properly specify the development of branchial and visceral MNs (Pattyn et al., 2003). In the pMN domain, Nkx6.1 and Nkx 6.2 activities are required for MN development, as loss of either transcription factors lead to loss of abducens and hypoglossal somatic MNs (Ericson et al., 1997; Sander et al., 2000; Vallstedt et al., 2001; Osumi et al., 1997). Loss-of-function of other genes described in SpMN progenitor domains such as Pax6 and Olig2 leads to anomalies in early somatic MN specification (Figure 1B) (Novitch et al., 2001; Lu et al., 2002; Osumi et al., 1997). These observation show that the somatic MN progenitor domain is specified along the dorso-ventral axis through coordinated actions of extrinsic and intrinsic programs.

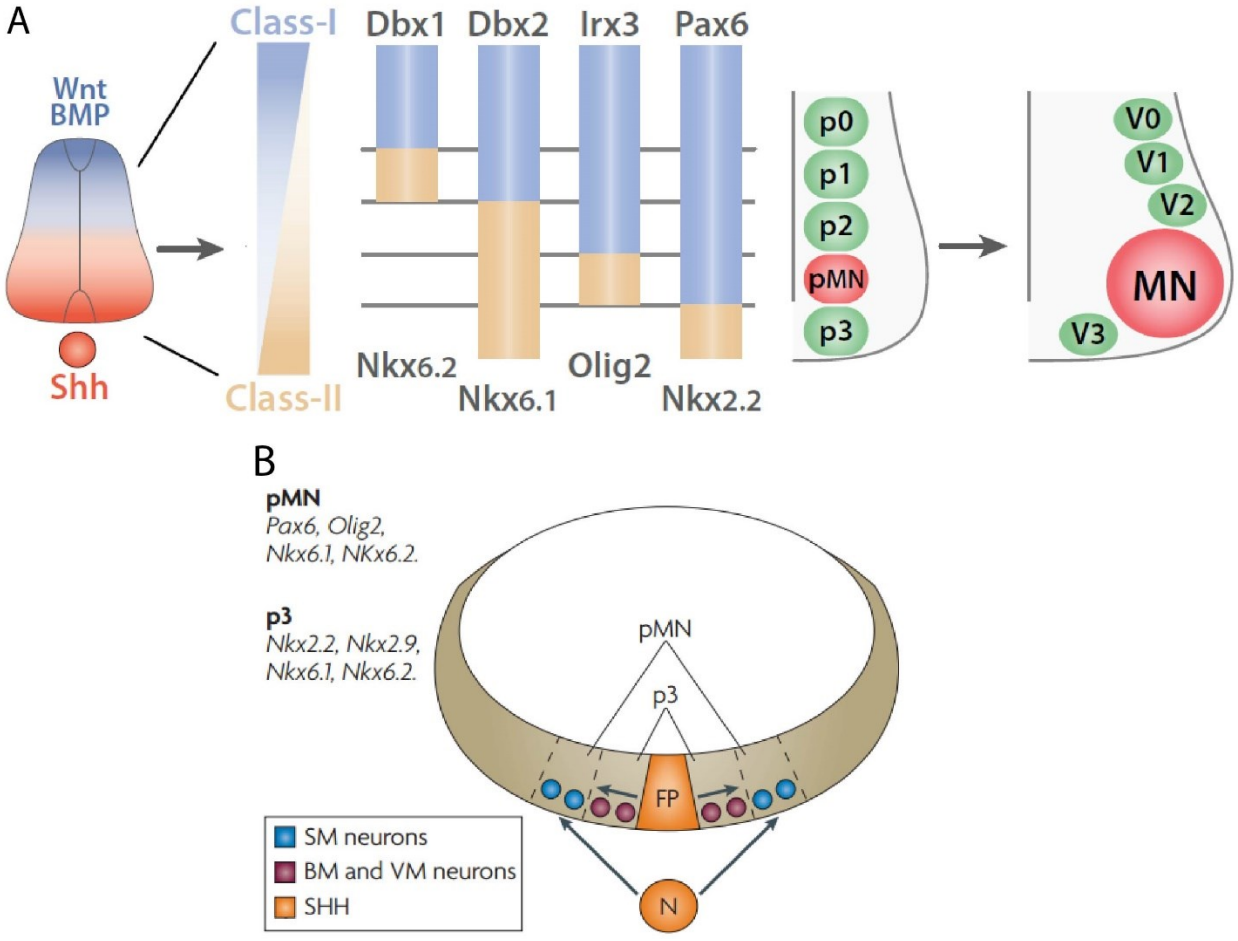

Figure 1. Dorso-ventral patterning of spinal cord and hindbrain. A) Figure as originally published in Stifani N (2013). Front. Cell. Neurosci. 8, 293. doi:10.3389/fncel.2014. A schematic representation of morphogen gradient in developing spinal cord. During development, Shh gradient is established in a ventral-high to dorsal-low pattern. Conversely, Wnt and BMP gradients are established ventral-low to dorsal-high. As a result of exposure to specific concentration of various morphogens, the ventral spinal cord expresses gradients of Class I and Class II transcription factors along the dorso-ventral axis. Class I transcription factors such as Dbx1, Dbx2, Irx3, and Pax6 are expressed more dorsally while class II transcription factors such as Nkx6.2, Nkx6.1, Olig2, and Nkx2.2 are express more ventrally. As a result of extrinsic and intrinsic patterning, the ventral progenitors are patterned into p0, p1, p2, and p3 domains that each gives rise to V0, V1, V2, and V3 interneurons, respectively. MNs are specified from pMN progenitor domain. B) Figure as originally published in Guthrie S (2007). Nat Rev Neurosci, 8(11), 859-871. doi:10.1038/nrn2254. Similar to the spinal cord, caudal hindbrain progenitors are patterned into two domains, p3 and pMN. Under the influence of various Class II transcription factors, pMN gives rise to somatic MNs. Meanwhile, p3 domain gives rise to branchial MNs and visceral MNs as a result of Class I transcription factor signaling.

[2.2.4] Transition from pMN progenitors to post-mitotic somatic motor neurons.

Following specification of the pMN domain, progenitors exit the cell cycle to give rise to mature somatic MNs that migrate laterally away from medial progenitors. This transition from progenitor to somatic MNs involves progenitors to exit the cell cycle, detach from the neuroepithelium, and enter the differentiation process to become post-mitotic MNs (Stifani, 2014; Kania, 2014). One of the key genes identified in this process is the transcriptional repressor Olig2, which was briefly mentioned previously as being expressed in the pMN domain. In the spinal cord and brainstem, Olig2 acts by contributing to the expression of a bHLH protein named neurogenin 2 (Ngn2) (Novitch et al., 2001; Lu et al., 2002; Zhou and Anderson, 2002). It has been further suggested that high concentration of Olig2 prevents premature expression of MN genes while accumulating concentration of Ngn2 allows a subset of $Olig2^{+}$ progenitors to

differentiate and activate post-mitotic MN programs (Lee et al., 2005). Through the combined transcriptional activity of Olig2 and Ngn2, MN progenitors leave cell cycle and express genes important for specifying postmitotic somatic MN fate, such as pancreas homebox 1 (Hb9) protein (Tanabe et al., 1998; Lee et al., 2005).

Following Hb9 expression, MNs become intrinsically competent to maintain post-mitotic MN-specific programs and maintenance is partly consolidated by ability of Hb9 to positively regulate its own expression. When Hb9 was genetically deleted in mice, MNs expressed interneuron markers and were found in abnormal locations within the spinal cord (Arber et al., 1999; Thaler et al., 1999). For such reason, Hb9 is used as a reliable marker to identify post-mitotic MNs in the literature, and in this paper. In addition to Hb9, developing MNs express other important groups of transcription factors such as LIM-homeobox genes Islet 1 (Isl1), Islet 2 (Isl2), Lhx3, and Lhx4 (Valera-Echavarria et al., 1996; Sharma et al., 1998; Thaler et al., 2002; Dasen and Jessell, 2009) Like Hb9, Isl1 and Isl2 are also used to label somatic MNs while transcriptionally regulating genes important for MN functions. For example, Drosophila Islet programs the electrical properties of specific group of MNs by regulating K+ channel expression (Wolfram et al., 2012). Isl1 is also expressed in post-mitotic branchial and visceral MNs, with the exception being that these MNs also express T-box transcription factor Tbx20 and paired-like homebox proteins Phox2a and Phox2b (Takeuchi et al., 2005; Brunet and Pattyn, 2002). Lhx3 and Lhx4 were shown to be determinants for proper development of ventrally exiting somatic MNs as inactivation of both genes results in loss of caudal somatic MNs of 12N and 6N (Sharma et al., 1998). In summary, pMN progenitors must exit cell cycle and initiate differentiation programs that are in part mediated by factors such as Olig2 and Ngn2 that promote expression of post-mitotic somatic MN genes such as Hb9 and Isl1.

[2.3] Development of somatic motor neuron topographic maps

Functional motor circuits are formed in part through the coordinated regulation of MN identity, cell body position, and target connectivity. After the expression of Hb9 is activated, MNs must further differentiate into specific subtypes identified by their ability to innervate specific muscle groups. Such functionally distinct subtypes are also identified by the unique topographic coordinates of their cell bodies in the ventral horn of the spinal cord and ventral half of the hindbrain (Guthrie, 2007; Stifani, 2014; Kania, 2014). In the case of SpMNs, subtypes of MNs are organized into distinct anatomical columns, called 'motor columns' along the rostro-caudal axis. There are six major columns described in the literature: preganglionic column (PGC), hypaxial motor column (HMC), median motor column (MMC), lateral motor column (LMC), phrenic motor column (PMC), and spinal accessory column (SAC) (Figure 2A) (Prasad and Hollyday, 1991; Tsuchida et al., 1994., Jessell, 2000; Dasen and Jessell, 2009; Kanning et al., 2010; Philippidou and Dasen, 2013; Francius and Clotman, 2014).

Each motor column is found in unique dorso-ventral as well as rostro-caudal coordinates and is characterized by a unique expression profile that provides genetic programs for consecutive steps of development such as axon projection pattern towards the periphery (Figure 2B and 2C). Motor columns can be further topologically subdivided into smaller groups of MNs, called 'pools,' that occupy unique topologic coordinates and innervate more specific muscle fiber groups within the general group of muscles innervated by the motor column. For example, SpMNs of the LMC innervate muscles of the limbs. LMC MNs can be further subdivided into medial LMC (LMCm) and lateral LMC (LMCl), which innervate ventral and dorsal limb musculatures, respectively, and occupy positions more medial and lateral within the LMC (Figure 2C) (Landmesser, 1978; Tosney and Landmesser, 1985; Dasen and Jessell, 2009; Kanning et al., 2010). In the case of 12N MNs, MN pools that innervate specific muscles of the tongue are also organized in developmentally organized patterns (Lewis et al. 1971; Krammer et al.

1979; Chibuzo and Cummings, 1982; Aldes 1995; Odutola 1976; Uemura-Sumi et al. 1981; McClung and Goldberg 1999, 2000). However, unlike SpMN, molecular expression profiles unique to each subtypes, or pools, of 12N MNs are yet to be identified.

[2.3.1] Hox proteins are important for motor neuron subtype specification along the rostro-caudal axis

As previously mentioned, different signaling programs along the rostro-caudal axis of the spinal cord result in development of topographically organized motor columns at cervical, thoracic, or lumbar levels of the spinal cord. Rostro-caudal positional specification of each column begins at similar developmental periods in parallel to generation of spinal MNs from the pMN domain as positional identity of neurons is established before the first differentiating neurons can be identified. In other words, positional identities are already programmed by MN progenitors and maintained throughout the emergence of post-mitotic MNs (Nordstrom et al., 2006; Francius and Clotman, 2014). A well-studied mechanism by which MNs are intrinsically patterned along the rostro-caudal axis is through non-overlapping expression of Hox proteins at different segments of the spinal cord in response to extrinsic signals (Dasen and Jessell, 2009; Philippidou and Dasen, 2013). Indeed, when expression of caudally expressed *Hox* genes, such as *HoxC*, was induced in more anterior regions by ectopic morphogens, such as FGF8, anterior brachial MNs were converted to more caudal thoracic MNs (Dasen et al., 2003). Conversely, when rostral brachial *Hox* genes were ectopically expressed in more caudal thoracic levels, rostral motor column identity, such as LMC fate, was promoted at the expense of rostral motor column cells, such as PGC cells (Lacombe et al., 2013). In summary, various *Hox* genes and their non-overlapping expression allows for generation of diversity of MNs along rostro-caudal axis of the spinal cord.

Hox genes have also been shown to be important for rostro-caudal generation and patterning of cranial MNs. The vertebrate hindbrain is divided into rhombomeres, which are segmental swellings evident during a transient time during development.

Cranial MNs found in different rhombomeres are in part patterned through *Hox* expression. In the hindbrain, *Hox* genes in paralogue groups 1 and 2 (*Hox* 1/2) are expressed in rostral and caudal rhombomeres while paralogue groups 3, 4, and 5 (*Hox* 3/4/5) are expressed only in caudal rhombomeres (Guthrie, 2007; Philippidou and Dasen, 2013, di Bonito et al., 2013). When rostrally expressed *Hox* genes are lost, patterning defects occurs such that rostral branchial and visceral MNs of the 5N and 7N are lost. Vice versa, somatic MNs in caudal rhomomeres are lost as a result of loss of group 3 *Hox* paralogues (Guthrie, 2007). In comparison to rostral cranial nuclei, more caudal nuclei are under the influence of multiple Hox proteins (Philippidou and Dasen, 2013). For example, abducens nucleus (i.e., 6N) MNs located in r5 are influenced by *Hox3* homologs and *Hoxa1* as loss of either gene group results in loss of 6N or 6N nerve (Mark et al., 1993; Gaufo et al., 2004; Guidato et al., 2003). In r6, *Hox3* genes coordinate MN development as 9N MNs exhibit defects in axon pathfinding in *Hox3* mutants (Manley and Capecchi, 1997; Watari et al., 2001). Additionally, lack of Hox3 expression also resulted in aberrant caudal migration of rostral 7N MNs in part due to loss of repression of Hoxb1 by Hox3 (Gaufo et al., 2003). Interestingly, *Hox4/5* paralogues are expressed in the caudal hindbrain r8 where somatic MNs of the 12N are specified, yet future studies are needed to identify the specific role of Hox4/5 in generation of 12N MNs (Guthrie, 2007, Di Meglio et al., 2013). In summary, vertebrate hindbrain cranial MNs are also patterned along the rostro-caudal axis in part by Hox-mediated mechanisms.

[2.3.2] Medio-lateral migration and settling of post-mitotic motor neurons

SpMNs migrate laterally away from the medial neuroepithelium and settle in ventral horns of the spinal cord. This migration is facilitated by the inherent structure of the spinal cord progenitors, whose cell soma is adjacent to the ventricular zone with long processes extending laterally, much reminiscent of radial glia. Indeed, spinal cord progenitors serve dual purpose as a source of newborn neurons but also as a scaffold for newborn SpMNs to migrate towards the ventral horn (Malatesta et al., 2000; Choi, 1981, Gomez et al., 1990; Kania, 2014).

Accurate SpMN migration towards lateral positions on a segmental level relies on expression of transcription factors such as Hox proteins and LIM homeodomain proteins (Kania, 2014). Hox proteins that are present during cell division serve to control medio-lateral MN soma settling positions in addition to rostro-caudal axis as discussed above. As an illustration, a study has shown that inhibiting Hoxc8 caused rostral shift in expression of more caudal Hox protein Hox5. As a consequence, a rostral pool of MNs innervating the *scapulohumeralis posterior* muscle exhibited shortened rostro-caudal length as the caudal domain of these MNs was lost due to dependency on Hoxc8-mediated genetic programs for specification. Meanwhile, caudal MNs innervating the *pectoralis* muscle under the influence of Hox5 expanded rostrally to form an ectopic domain. More importantly, post-mitotic settling positions were affected as the ectopic pool of *pectoralis* MNs settled in medio-lateral coordinates unique to endogenous domain of MNs innervating *pectoralis* muscle, visualized by *pectoralis* MN marker Pea3 transcription factor (Dasen et al., 2005; Kania, 2014). Similarly, loss of another *Hox* gene, *Hox6,* expressed in brachial spinal cord leads to defects in $Pea3^{+}$ LMC MNs (Lacombe et al., 2013). At later time periods after differentiation of MN progenitors, LIM homeodomain proteins such as Lhx3 and Lhx1 become important for MN medio-lateral settling positions. In the chick spinal cord, ectopic expression of a medial protein Lim3 (i.e., chick Lhx3 homologue that marks MMC) in LMC MNs induced LMC MNs to settle in more medial locations (Sharma et al., 2000). Similarly, forced expression of lateral protein Lim1 (i.e., chick Lhx1) that marks LMCl in more medially located LMCm caused LMCm to settle in more lateral positions within the LMC (Kania and Jessell, 2003). Taken together, transcriptional regulations through Hox proteins and LIM homeodomain proteins are important molecular mechanisms for SpMN soma settling along the medio-lateral axis.

Similar to SpMNs, 12N MNs are also under the influence of various transcription factors that regulate specification along the three axes: rostro-caudal, dorso-ventral, medio-lateral. However, most molecular studies of 12N development focused on early stages of 12N MN development. At later stages, there is a paucity of information on the establishment and maintenance of 12N MN somatotopic maps. Before we can address

how 12N MN somatotopic map can be studied, we shall discuss how the 12N somatotopic map is wired to the muscles of the tongue.

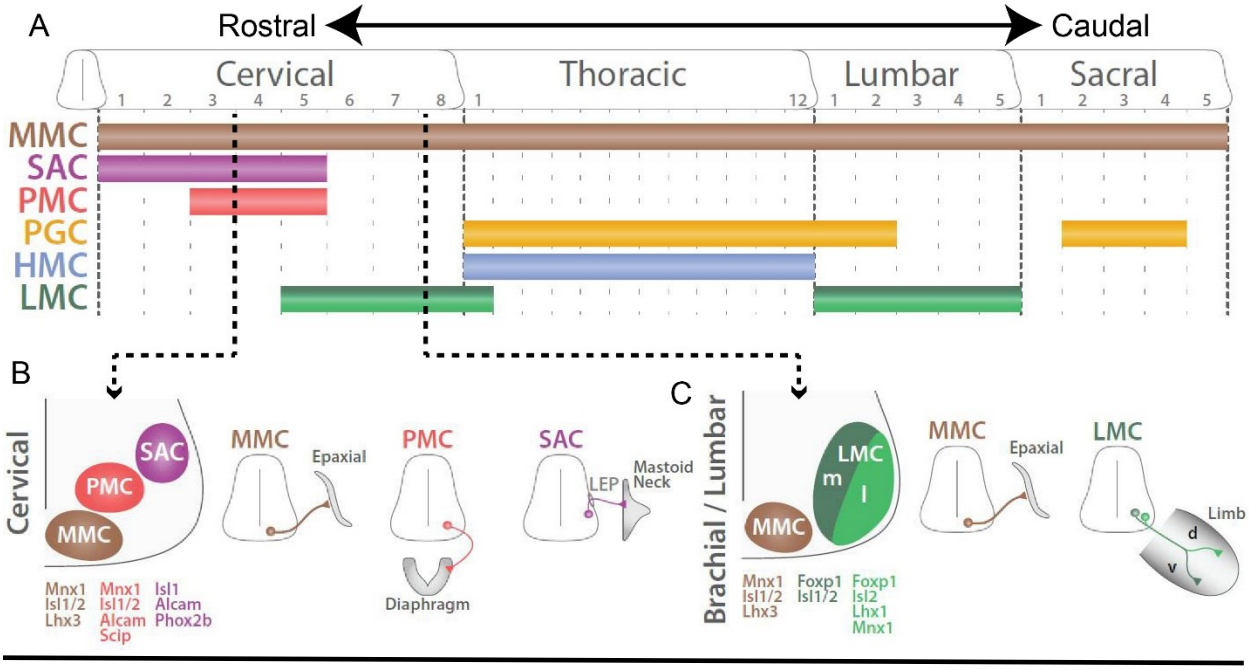

Figure 2. Vertebrate SpMN somatotopic organization Figure adapted from Stifani N (2013). Front. Cell. Neurosci. 8, 293. doi:10.3389/fncel.2014. A) Along the rostro-caudal axis, the spinal cord can be divided into cervical, thoracic, lumbar, and sacral segments. There are multiple motor columns spread out through the rosto-caudal axis of the spinal cord. MMC is found throughout the entire spinal cord. SAC is found from C1 to C5. PMC is located between C3 and C5. LMC is found from C5 to T1. In the thoracic spinal cord, PGC is found from T1 to L2 while HMC is located from T1 to T12. In the Lumbar and Sacral spinal cord, LMC is found from L1 to L5 while PGC is located from S2 to S4. B) At cross sectional level C3 and C4, MMC is most medially situated while PMC is found between MMC and the more lateral SAC. MNs of MMC express Mnx1/Hb9, Isl1/2 and Lhx3 in their post-mitotic somatotopic positions and innervate hypaxial muscles involved in postural movement. MNs of the PMC are characterized by their innervation of the diaphragm and expression of transcription factors Mnx1/Hb9, Isl1/2, Alcam and SCIP. SAC innervates mastoid muscle and is distinguished by its expression of Phox2b and lack of expression of Mnx1/Hb9. C) At cross sectional level C6 to C8, the MMC is

located in a medial location within the ventral horn, similar to other segments of the spinal cord. MNs of the LMC are found lateral to the MMC; they are characterized by the expression of FoxP1 and Isl2 and by the innervation of muscles of the limbs. The LMC may be further subdivided based on anatomical functions and molecular profiles. LMCm is more medially located within the LMC, innervates ventral muscles of the limb, and expresses Isl1. In contrast, LMCl does not express Isl1 but expresses Mnx1/Hb9 and Lhx1. LMCl can be further characterized by its lateral topographic position within the LMC and its innervation of dorsal muscles of the limb.

[2.4] Motor neurons of the hypoglossal nucleus

[2.4.1] Different hypoglossal motor neurons innervate different muscles of the tongue

The motor circuit comprising 12N MNs in the hindbrain and muscles in the tongue is an essential biological network given the involvement of the tongue in vital functions such as chewing, swallowing, and breathing (Lowe 1980, 1984; Sawczuk & Mosier, 2001; Fregosi, 2011). 12N MNs innervate two main tongue muscle groups that are anatomically defined as either intrinsic or extrinsic. Intrinsic muscles have both origin and insertion within other muscles of the tongue and control fine movements of the tongue involved in speaking, eating, and swallowing (Sonntag, 1925). Extrinsic muscles have one end attached to a bone with the other end inserting into the base of the tongue. Extrinsic muscles control postural movements affecting tongue position and are situated within the mouth while intrinsic muscles may be situated to function outside the mouth and comprise the bulk of the tongue. However, the anatomical separation between intrinsic and extrinsic muscles of the tongue may not be visually clear as both muscle groups interdigitate and act together during most tongue movements (Hellstrand, 1980; Sokoloff and Deacon, 1992; Smith et al., 2005).

Extrinsic muscles may be further classified into two categories by their function. Extrinsic muscles that are used to protrude the tongue are called ‘extrinsic protrusor’ muscles while extrinsic muscles used for retraction of the tongue are called ‘extrinsic retractor’ muscles. Similarly, different intrinsic tongue muscles are also often referred to as either protrusors or retrusors, although various intrinsic muscles are active, to varying degrees, during both protrusion and retraction. All of the tongue muscles are involved in the precise execution of the large number of actions performed by the tongue (Aldes 1995; Altschuler et al. 1994; McClung and Goldberg 1999, 2000; Lowe 1981, 1984).

[2.4.2] Somatotopic organization of hypoglossal motor neurons

In most mammalian species, 12N has a characteristic 'somatotopic organization' in which MNs innervating protrusor or retrusor muscles are functionally segregated into defined positions along the three body axes (Figure 3). Observations obtained from retrograde axonal labelling experiments have identified dorsal and ventral compartments of the 12N. MNs located in the dorsal half of 12N generally innervate retrusor muscles and are found in the rostral 2/3 of the nucleus. Ventral 12N MNs found in the caudal 2/3 of the nucleus mostly innervate protrusor muscles (McClung and Goldberg, 1999). The ventral 12N compartment is further subdivided into medial and lateral components: ventromedial and ventrolateral 12N. Ventromedial 12N MNs innervate intrinsic protrusor muscles of the tongue (e.g., transversus and verticalis) while ventrolateral 12N MNs innervate extrinsic protrusor muscles of the tongue (e.g. genioglossus). Likewise, dorsal 12N is also divided along the medio-lateral axis into two compartments: dorsomedial and dorsolateral. Dorsomedial MNs innervate instrinsic retrusors (e.g., superior longitudinal and inferior longitudinal) while dorsolateral MNs innervate extrinsic retrusors (e.g., hyoglossus and styloglossus) (Figure. 3) (Lewis et al. 1971; Krammer et al. 1979; Chibuzo and Cummings, 1982; Aldes 1995;; Odutola 1976; Uemura-Sumi et al. 1981; McClung and Goldberg 1999, 2000). Anatomically, the human tongue shares a similar organization to that of the murine tongue with all major intrinsic and extrinsic muscle groups conserved between the two, raising considerable research interests in studying murine 12N MN development and innervation as a model.

The establishment of a precise 12N myotopic organization is essential to the formation of functional 12N MN-tongue musculature motor circuits. However, little is presently known about the molecular mechanisms controlling 12N MN somatotopic map formation during development.

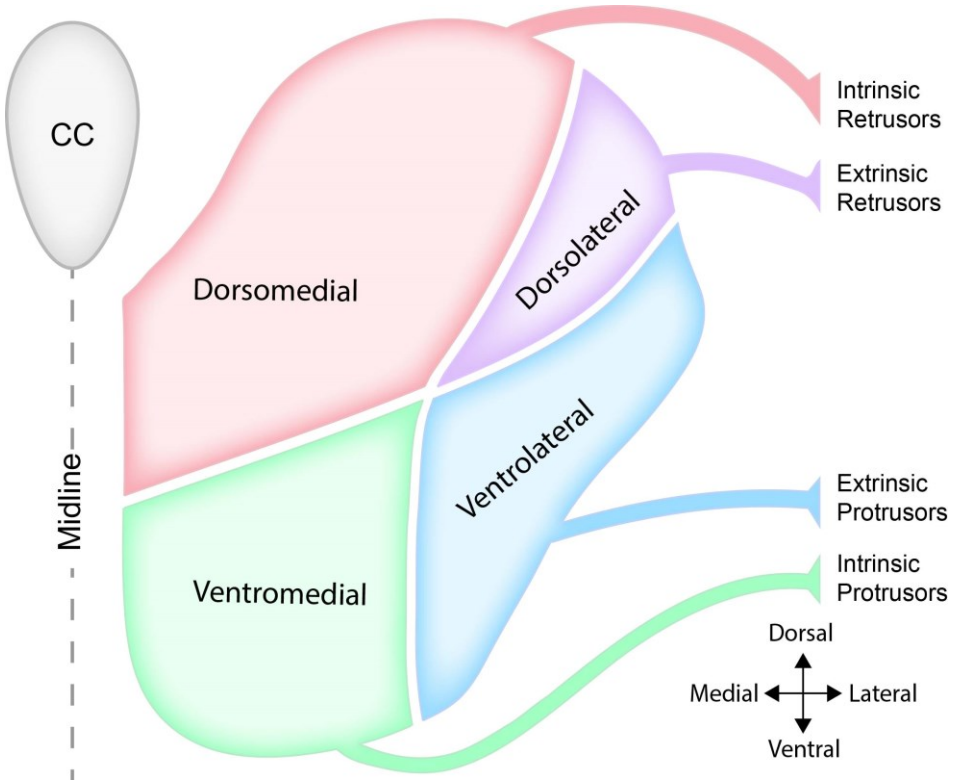

Figure 3. 12N somatotopic map (Figure adapted from Chen X, Wang J. W, Salin-Cantegrel A, Dali R, & Stifani S. (2015). Brain Struct Funct. doi:10.1007/s00429-015-1160-2). A schematic of compartmental organization of 12N MNs and their axonal targets. Along the dorsoventral axis, dorsal 12N MNs innervate retrusor muscles of the tongue while ventral 12N MNs innervate protrusor muscles. The distribution of dorsal and ventral MN varies along the rostrocaudal axis as the majority of dorsal and ventral MNs are found in rostral and caudal 12N, respectively (not shown in figure). Along the mediolateral axis, medial (towards the midline) 12N MNs innervate intrinsic muscles while lateral 12N MNs innervate extrinsic muscles. CC, central canal.

[2.5] Runx1, FoxP1, and SCIP: three transcription factors important for motor neuron development

In somatotopic MN development, a number of transcription factors play important roles in subtype specification, soma body positioning, and axonal targeting along the three axes. Here, we shall highlight the roles of three particular transcription factors, Runx1, FoxP1, and SCIP, describing examples of their roles during the development of MNs and other neuronal cells.

[2.5.1] Runx family in neuronal development

Previous studies in the developing murine spinal cord and hindbrain revealed that Runt-related transcription factor 1 (Runx1) is expressed in certain groups of branchial, visceral and somatic MNs, including MNs of the 12N (Theriault et al., 2004, Stifani et al., 2008; Chen et al., 2015; Yoshikawa et al., 2015). Unlike early Hox proteins or Class I and Class II proteins, Runx1 is not expressed in MN progenitors. Instead, it was shown to be expressed in post-mitotic MNs acquiring topology and/or establishing axonal connections (Stifani et al., 2008). Though the specific role of Runx1 in acquisition of topology and axonal connection of MNs is yet to be explored in depth, we may refer to demonstrated roles of Runx1 in the peripheral nervous system (PNS) to infer how Runx1 may contribute to MN development.

In the PNS, Runx1 is a well-known regulator of specific sensory neuronal subtype identity and axon targeting. Specifically, during DRG development, Runx1 is preferentially expressed in a subset of nociceptive neurons that are involved in sensation of pain, itch, and temperature. Initially, during prenatal stages, most nociceptive DRG sensory neurons express both tyrosine kinase receptor A (TrkA) and Runx1 (Levanon et al., 2002; Chen et al., 2006; Kramer et al., 2006). However, during perinatal and postnatal stages, approximately half of the initially $TrkA^{+}Runx1^{+}$ neurons express either TrkA or Runx1, giving rise to two different subtypes of nociceptors called

peptidergic (Runx1-negative) and non-peptidergic (Runx1-positive), respectively. During this divergence, Runx1 is thought to repress the expression of peptidergic-specific genes such as calcitonin-gene-related-peptide (CGRP), TrkA, and mu-class opioid receptor (Chen et al., 2006; Kramer et al., 2006; Yoshikawa et al., 2007). In addition to specifying subtypes, Runx1 also regulates the axon trajectory of DRG sensory neurons. When Runx1 is inactivated, Runx1+ non-peptidergic neurons send their axons along targets of peptidergic neurons. Vice versa, ectopic expression of Runx1 in TrkA+ peptidergic neurons causes these neurons to innervate non-peptidergic neuron targets (Chen et al., 2006; Kramer et al., 2006; Yoshikawa et al., 2007). More specifically, Runx1 is associated with proper specification of neurons innervating skin epidermis, hair follicles, and subsets of mechanoreceptors (Chen et al., 2006; Yoshikawa et al., 2007; Yang et al., 2013; Moqrich, 2014; Lou et al., 2013; Lou et al., 2015).

During the development of proprioceptive neurons, another Runx family member, Runx3, coordinates segregation of neuronal lineages. Proprioceptive neurons are derived from transiently existing population of $TrkB^+/TrkC^+$ precursors. At a later time period, Runx3 expression begins in $TrkC^+$ proprioceptive neurons when $TrkC^+$ neurons no longer express TrkB, a marker of mechanoreceptive neurons. Runx3 deficiency in mice leads to decrease in number of $TrkC^+$ neurons and neurons expressing Parvalbumin (PV), a marker of proprioceptive neurons. This loss of $TrkC^+$ neurons does not seem to be due to increased cell death, but rather to concomitant increase of $TrkB^+$ neurons (Inoue et al., 2002; Levanon et al., 2002; Kramer et al., 2006; Inoue et al., 2007; Nakamura et al., 2008; Lallemend et al., 2012). Conversely, ectopic expression of Runx3 in $TrkB^+$ neurons lead to decrease in $TrkB^+$ neurons, possibly due to direct transcriptional regulation by Runx3 of *TrkB* intronic regulatory elements (Kramer et al., 2006; Inoue et al., 2007). In addition to its roles in segregation of proprioceptive vs mechanoreceptive lineages, Runx3 is also involved in development of correct axon targeting of sensory neurons. For example, Runx3 controls expression levels of cytoplasmic proteins Rock1 and Rock2 involved in axon extension of early sensory neurons (Lallemend et al., 2012). Consistently, Runx3 loss-of-function and ectopic gain-of-function studies in DRG sensory neurons show defects in establishment of proper

connections (Inoue et al., 2002; Levanon et al., 2002; Chen et al., 2006; Kramer et al., 2006; Nakamura et al., 2008).

The observation that Runx family members play important roles in specific sensory neuronal subtype identity and axon targeting suggests that they might play similar roles in other neuron types. In agreement with this possibility, Runx1 is expressed in spinal cord MNs during embryonic stages when these cells are acquiring topology and establishing axonal innervations (Stifani et al., 2008). Thus, one of the main aims of this Thesis was to address the hypothesis that Runx1 may be expressed, and play a role, during the development of 12N MNs.

[2.5.2] Transcription factor FoxP1 in motor neuron development

One of the modes of action proposed for Hox proteins during MN development is that Hox proteins of brachial and lumbar segments are dependent on the forkhead box transcription factor FoxP1 for the expression of all LMC pool determinants (Dasen et al., 2008; Rousso et al., 2008; Palmesino et al., 2010; Philippidou and Dasen, 2013; Davis-dusenbury et al., 2014). FoxP1 is expressed in all LMC MNs and is therefore utilized as marker of the LMC fate (Figure 2C). During brachial spinal cord development, various Hox proteins such as Hox6 and Hox10 induce the expression of FoxP1, which in turn cooperates with Hox proteins to induce LMC-specific developmental programs while repressing thoracic MN-specific programs (Dasen et al., 2008; Rousso et al., 2008). *Foxp1* loss-of-function experiments showed developmental consequences in LMC development. Specifically, *Foxp1* mouse mutants developed general spinal MN at the topographic location where the LMC is normally specified. However, these MNs did not express the typical profiles of LMC MNs and retrograde labelling experiments suggested that the smaller pools of MNs innervating specific muscle fibers were not myotopically organized (Dasen et al., 2008; Rousso et al., 2008). A possible explanation for loss of somatotopic organization may be attributed to cadherin family of adhesion molecules as they are lost in *Foxp1*-/- mice (Dasen et al., 2008; Demireva et al., 2011). Further evidence suggests that scrambling of somatotopic map due loss of *Foxp1* may have affected the specificity of the sensory-motor circuit as prioprioceptive neurons of the DRG connected to traditional locations within the ventral horn regardless of

scrambled MN map in *Foxp1*-/- mice (Surmeli et al., 2011). The importance of FoxP1 in specifying the LMC fate is further suggested by in vitro embryonic stem cell differentiation experiments in which forced expression of FoxP1 generated a significant increase in the proportion of LMC neurons. Additionally, upon transplantation into developing chick spinal cord, *in vitro*-generated LMC neurons, under forced expression of FoxP1, integrated into motor circuits innervating muscles of the limb (Adams et al., 2015). Given the critical importance of FoxP1 for LMC somatotopic organization and circuit formation, it is not surprising that certain *Hox* genes, such as *Hoxc9*, promote thoracic developmental programs by either direct or indirect repression of *Foxp1* (Jung et al., 2014).

[2.5.3] Transcription factor SCIP in motor neuron development

Another subtype of MNs that are closely located to FoxP1-expressing LMC MNs are the MNs of the PMC (Figure 2A). Interestingly, in contrast to limb-level brachial Hox-dependant MN subtypes that are lost in *Foxp1* mutants, PMC neurons increase in number when *Foxp1* is inactivated (Rousso et al., 2008). PMC MNs, located in the cervical spinal cord, innervate the diaphragm, which is a vital muscle given that it carries out the majority of the respiratory function in mammals. Molecularly, PMC MNs are characterized by expression of the POU-domain transcription factor SCIP, also known as Pou3f1 or Oct-6 (Figure 2B) (Philippidou et al., 2012). A previous study demonstrated that *hox5* gene expression is necessary for proper PMC development as *hox5* mutants showed disturbed organization, survival, and patterns of target innervation (Philippidou et al., 2012) Interestingly, SCIP expression was unaltered in *hox5* mutants, raising further questions as to the roles of SCIP in PMC development (Philippidou et al., 2012). To further characterize the role of SCIP in PMC development, an *in vitro* gain-of-function study induced the expression of SCIP alone or in combination with other PMC development regulators in MNs differentiated from embryonic stem cells. This study revealed that SCIP is downstream of Notch signaling and that it acts in combination with Hoxa5 to regulate like-like clustering of PMC-like neurons *in vitro* possibly through regulating downstream cadherin effectors such as Pch10 and Cdh10 (Machado et al., 2014). In the brachial spinal cord, SCIP is also

expressed in subset of LMC neurons innervating *flexor carpi ulnaris* muscle (Dasen et al., 2005). Like Runx family members, POU-domain transcription factors, such as Brn3a (Pou4f1), also contribute to sensory circuit development. Past studies in sensory development in the DRG and trigeminal ganglion (TG) have shown that Brn3a/Pou4f1 plays important roles in neuronal specification, differentiation, and axonal targeting (Eng et al., 2007; Lanier et al., 2009; Dykes et al., 2010; Badea et al., 2012; Zou et al., 2012). Notably, Pou4f1 regulates sensory neuron specification by positively regulating the expression of Runx1 and Runx3, as loss of Pou4f1 lead to significant downregulated of Runx1/3 and consequent downstream Runx effectors such as Trk neurotrophin receptors and CGRP (Dykes et al., 2010; Zou et al., 2012). The observation that POU-domain transcription factors such as SCIP and Brn3a play important roles in MN and sensory neuron subtype identity suggests that they might also play similar roles in 12N MN development. In agreement with this possibility, SCIP is robustly expressed in the 12N and mice with genetic deletion of SCIP exhibit fatal respiratory defects, possibly due to perturbations in 12N and PMC respiration-related motor circuits (Birmingham et al., 1996). Additionally, non-overlapping expression pattern between SCIP and other known regulators of neuronal subtype development, such as FoxP1, also makes SCIP an attractive gene for investigation, especially considering POU-domain transcription factors regulate Runx family members during sensory development.

[2.6] Rationale and Objectives

The establishment of topographic patterning of MN diversity in the vertebrate spinal cord has been the subject of numerous investigations. In comparison, studies of the topographic development of 12N MNs are scarce. Given the biological importance of 12N motor circuit in regulating vital motor processes, understanding how 12N MN diversity is generated and maintained, and how these neurons perform their functions, attracts considerable research interests. Based on these considerations, studies presented in this thesis had two main aims.

First, to characterize the molecular profiles of specific 12N MN subtypes that had been previously defined anatomically. The aim was to characterize the expression of specific genes previously used as markers of developing SpMN pools and sensory neuron subtypes, including genes under Runx1-mediated transcriptional regulation.

Second, to understand the role of specific transcription factors whose expression marks separate 12N MN populations in the establishment and maintenance of 12N MN somatotopic map. Specifically, we hypothesized that restricted and possibly mutually-exclusive expression of certain transcription factors may serve roles in regulating transcriptional programs unique to separate 12N MN subtypes and delineating 12N topographic boundaries.

[2.7] Previous work and rationale

[2.7.1] Runx1 is expressed in ventromedial hypoglossal motor neurons innervating intrinsic tongue muscles

Runx1 is expressed in restricted populations of somatic MNs in the developing mouse cervical spinal cord and 12N (Stifani et al. 2008; Yoshikawa et al. 2015). To characterize the spatiotemporal pattern of *Runx1* during 12N development, our lab took advantage of mice in which the bacterial *LacZ* gene was knocked into the *Runx1* locus (*Runx1*^{LacZ} mice), resulting in the expression of a nuclear form of βGalactosidase (βGal) under the control of the *Runx1* promoter (North et al. 1999). *Runx1*^{LacZ} mice exhibit a pattern of βGal expression in the nervous system that faithfully reproduces the expression of the endogenous Runx1 protein (Murthy et al. 2014; Stifani et al. 2008; Zagami and Stifani 2010; Zusso et al. 2012).

At embryonic stages E11.5–E12.5, when 12N MNs start to assemble into a detectable nucleus, *Runx1*^{LacZ} mouse embryos exhibited robust βGal enzymatic activity in Phox2b-expressing visceral 10N MNs dorsal to Hb9-expressing 12N MNs (not shown here but described in Chen et al., 2015). At E14.5, βGal expression became detectable in two symmetrical groups of cells along the midline expressing the MN markers choline acetyl transferase, Isl1, and Hb9, indicating that these βGal^{+} cells were 12N somatic MNs (Chen et al., 2015). βGal expression in the 12N persisted throughout embryonic development (starting at approximately E13.5) into early adulthood in *Runx1*^{LacZ} mice. During all stages, immunofluorescence double-labelling studies showed βGal expression was an accurate recapitulation of Runx1 protein expression (Chen et al., 2015).

Along the rostro-caudal axis of 12N, little or no *Runx1* expression was found in the rostral half of 12N (Chen et al., 2015). The majority of 12N cells coexpressing Isl1

and βGal occupied a ventromedial position within the caudal 12N of *Runx1*^{LacZ} mice (Chen et al., 2015; summarized in Figure 4). Runx1 continued to be preferentially expressed in the ventromedial quadrant of caudal 12N throughout embryonic development. Retrograde axonal labeling studies in which rhodamine conjugated dextran was injected into the anterior tip of the tongue, which is mostly composed of intrinsic muscles (Chibuzo and Cummings 1982; Krammer et al. 1979; Smith et al. 2005), showed that most, if not all, ventromedial βGal^{+} 12N cells were retrogradely labeled in *Runx1*^{LacZ} embryos, indicating that Runx1^{+} 12N MNs extend axons to intrinsic lingual muscles (Chen et al., 2015). Together, these findings show that Runx1 is preferentially expressed in intrinsic tongue muscle-innervating MNs in the ventromedial region of caudal 12N. These findings, which were mainly the result of work performed by Dr. Xin Chen, before my arrival to the Stifani lab, represented one of the main motivations of the studies of this M.Sc Thesis.

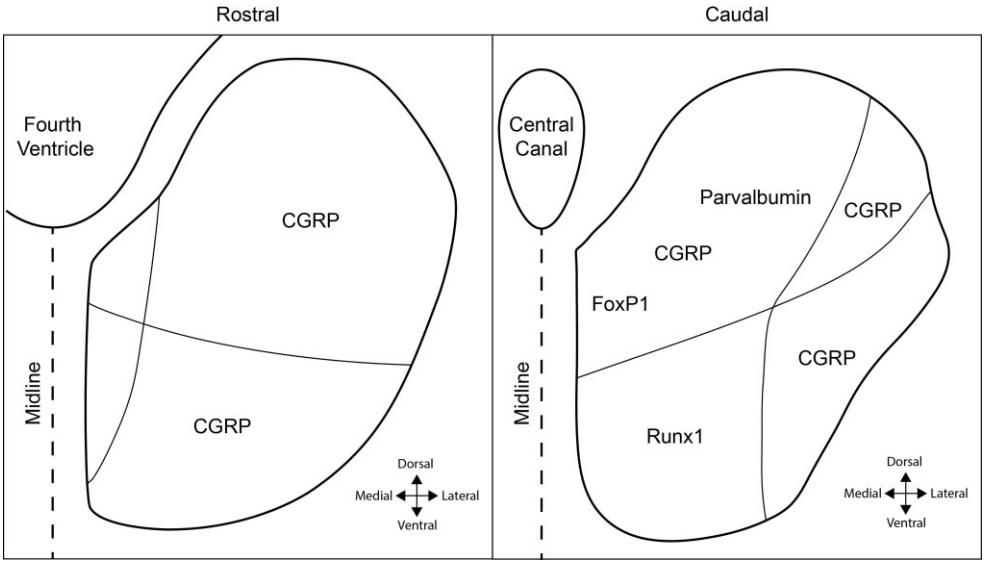

Figure 4. Schematic summary of the characterization of protein expression patterns in developing mouse embryo hypoglossal nucleus conducted prior to the start of my studies (Figure adapted from Chen X, Wang J. W, Salin-Cantegrel A, Dali R, & Stifani S. (2015). Brain Struct Funct. doi:10.1007/s00429-015-1160-2). Left-hand side: little or no expression of transcription factors Runx1 and FoxP1 is observed in the rostral part of the mouse 12N during embryonic development. CGRP is robustly

expressed in the rostral 12N region, Right-hand side: expression of Runx1 and FoxP1 is mainly observed in the caudal half of 12N, where their combined expression defines dorsomedial and ventromedial 12N domains (delimited by solid lines). These MN groups also exhibit specific patterns of CGRP and PV expression.

[2.7.2] Non-overlapping expression of Runx1, calcium binding proteins and neurotransmitters defines separate hypoglossal motor neuron groups

The restricted pattern of Runx1 expression in ventromedial MNs in caudal 12N prompted us to further characterize the molecular properties of this particular MN group. Previous studies have suggested that the neuropeptide calcitonin gene related peptide (CGRP) is mainly expressed in the rostral part of mammalian 12N (de Souza et al. 2008; Sienkiewicz et al. 2010). We therefore examined whether caudally located Runx1^{+} 12N MNs might express little or no CGRP, a possibility also consistent with the demonstration that Runx1 negatively regulates CGRP expression in the PNS (Chen et al. 2006; Kramer et al. 2006). CGRP was robustly expressed in almost the entire rostral 12N, where Runx1 is not considerably expressed. In caudal 12N of Runx1^{LacZ} embryos, CGRP was preferentially detected in dorsal and ventrolateral cells that were mostly devoid of βGal expression. The lack of significant overlap of Runx1 and CGRP was observed from E14.5 to E18.5 (Chen et al., 2015; summarized in Figure 4).

The observation of non-overlapping expression between *Runx1* and CGRP prompted us to test for the expression of other neural molecules that have been previously shown to be related to CGRP expression. CGRP is coexpressed with the calcium-binding protein Parvalbumin (PV) in some MNs in the canine spinal cord (Chang et al. 2008). In E16.5 and E18.5 embryos, PV expression was detectable in caudal 12N neurons dorsal to ventromedial βGal^{+} MNs (Chen et al., 2015). No detectable overlap between PV and βGal^{+} was observed, consistent with the previous demonstration that the activity of the Runx family member Runx3 is negatively correlated with PV expression in the mouse PNS (Levanon et al. 2002). A close comparison with CGRP expression revealed that a group CGRP+ cells that are dorsomedially located co-expressed PV (Figure 5; data obtained by this M.Sc. Thesis

candidate). Taken together, these observations provide evidence that the combinatorial expression of Runx1, CGRP, and PV defines separate groups of MNs located in at least two separate anatomical regions in the developing mouse 12N. They suggest further that Runx1^{+} ventromedial MNs in the caudal 12N do not use CGRP as a neurotransmitter and do not use PV as a calcium-buffering protein. These results, which were mostly the work of Dr. Xin Chen represented another observation that motivated the studies described in this Thesis.

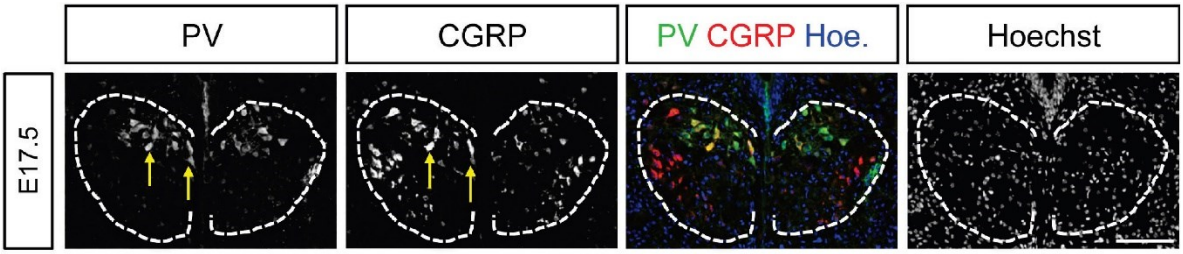

Figure 5. Expression of PV and CGRP in E17.5 mouse embryo hypoglossal nucleus. Representative double-labeling immunofluorescence analysis of PV and CGRP expression in 12N of E17.5 embryos. White curved dotted lines roughly demarcate the perimeter of 12N. Arrows point to examples of double-labeled cells in the dorsomedial compartment of 12N. CGRP^{+} cells that do not express PV can be observed in more lateral positions. Scale bar, 100 μm.

[2.7.3] Expression of Runx1 and transcription factors FoxP1 is correlated with hypoglossal motor neuron somatotopic organization

To further characterize the molecular profiles of Runx1^{+} and Runx1^{-} 12N MN groups, we compared Runx1 expression during 12N development to that of the transcription factor FoxP1. As mentioned above, FoxP1 plays an important role in the regulation of MN subtype development in the spinal cord (Dasen et al. 2008; Palmesino et al. 2010; Rousso et al. 2008; Surmeli et al. 2011). Runx1 represses transcription of the related *Foxp* family member *Foxp3* in hematopoietic cells (Bruno et al. 2009; Kitoh

et al. 2009; Rudra et al. 2009). Moreover, consensus Runx binding sites are present in the mouse *Foxp1* locus (studies by Ms. Rola Dali; published in Chen et al., 2015). Consistently, chromatin immunoprecipitation data suggesting binding of RUNX family proteins to the FOXP1 promoter in human cells is provided by the publicly available Encyclopedia of DNA Elements (ENCODE) Project (http://genome.ucsc.edu/ENCODE/) (Dunham et al. 2012) (Chen et al., 2015). These observations suggest that Runx1 may be involved in the regulation on *Foxp1* expression.

We observed that FoxP1 was preferentially expressed in caudal 12N. In contrast to Runx1, however, at all stages examined FoxP1 immunoreactivity marked mainly dorsomedial 12N cells that were for the most part separate from the βGal^{+} MNs located in ventromedial 12N of $Runx1^{LacZ}$ embryos. Most, if not all, FoxP1-expressing dorsomedial neurons in caudal 12N coexpressed PV, suggesting that they also coexpress CGRP based on the overlap of PV and CGRP in this region, as described above. A few cells coexpressing FoxP1 and Runx1 were also detected in the most medial part of the Runx1 expression domain, possibly representing a separate ventral 12N MN (sub)group or corresponding to cells in which a non-overlapping pattern of Runx1 and FoxP1 expression may occur only transiently during development. Together, these observations suggest that separate groups of cells expressing either FoxP1 (and PV) or Runx1 define two distinct populations of dorsomedial or ventromedial MNs in the caudal part of 12N, respectively (Chen et al., 2015; summarized in Figure 4). These studies, which were started by Dr. Xin Chen and continued in part by myself, also provided rationale for my own graduate studies.

In summary, our initial work molecularly characterized two separate previously-identified anatomical domains of 12N MNs: ventromedial ($Runx1^{+}$, $FoxP1^{-}$, PV^{-}, $CGRP^{-}$) and dorsomedial ($Runx1^{-}$, $FoxP1^{+}$, PV^{+}, $CGRP^{+}$) (Chen et al., 2015). Based on these observations, the present M.Sc. Thesis work had the following aims:

1) To further characterize the molecular profile of ventromedial and ventrolateral groups of 12N MNs.
2) To understand the role of specific transcription factors, including Runx1 and FoxP1, in the establishment and maintenance of 12N MN somatotopic map.

Chapter 3: Materials and Methods

Animal procedures

Runx1^{LacZ} knock-in mice were generated (North et al.1999) and genotyped (Theriault et al. 2005) as previously described. The recombined locus of Runx1^{LacZ} mice encodes a fusion protein of the N-terminal 242 amino acids of Runx1, containing a nuclear localization sequence, and bacterial βGal. As a result, the βGal containing fusion protein expressed in Runx1^{LacZ} mice is localized to the nucleus. Tau-lox-STOP-lox-Runx1-IRES-NLS-LacZ-pA (Tau^{Runx1}) knock-in mice were generated and genotyped as described (Kramer et al. 2006). To achieve conditional ectopic expression of Runx1 in MNs, Tau^{Runx1} mice were crossed with mice expressing Cre recombinase under the control of the MN *Hb9* gene promoter (Hb9^{Cre} mice) (Yang et al. 2001) to conditionally express Runx1 and βGal in somatic MNs (Kramer et al. 2006). Runx1^{LacZ}, Tau^{Runx1}, and Tau^{Runx1};Hb9^{Cre} embryos and pups were analyzed by histology, immunohistochemistry, and retrograde axonal labeling, as appropriate (n=3 for all genotypes and embryonic stages tested). For embryonic staging, the day of appearance of a vaginal plug was considered to be E0.5. All animal procedures were conducted in accordance with the guidelines of the Canadian Council for Animal Care and were approved by the Animal Care Committee of the Montreal Neurological Institute of McGill University.

Histology

Runx1^{LacZ} embryos were recovered, fixed in 2% PLP (0.075M L-lysine, 0.37M sodium phosphate, 2% Paraformaldehyde), dehydrated in 30% sucrose, and cryostat sectioned

at -28 °C as described (Theriault et al. 2005). βGal activity in Runx1^{LacZ} embryos was detected histochemically by rinsing sections from staged embryos three times in solution A (80 mM Na_2HPO_4, 20 mM NaH_2PO_4, pH 7.4, 2 mM $MgCl_2$, 0.2 % IGEPAL, 0.1 % sodium deoxycholate), followed by incubation for approximately 16 h at 37 °C in solution A containing 5 mM potassium ferricyanide, 5 mM potassium ferrocyanide, and 1 mg/ml 5-bromo-4-chloro-3-indolyl-b-galactopyranoside (XGal) (Invitrogen, Burlington, ON, Canada). Sections were then rinsed in phosphate buffered saline (PBS) and counterstained with eosin.

Immunohistochemistry

Sections from staged Runx1^{LacZ}, Tau^{Runx1}, and Tau^{Runx1}; Hb9^{Cre} embryos were rinsed in HEPES-buffered saline (HBS) and then pre-incubated for one hour in blocking solution, which consisted of 5 % normal donkey serum (Jackson ImmunoResearch Laboratories, West Grove, PA), 0.1 % Triton-X-100, and 0.5 mg/ml bovine serum albumin (Sigma-Aldrich, St. Louis, MO, USA) in HBS. Sections were incubated for approximately 16 h at 4 °C in blocking solution containing the following primary antibodies: rabbit anti-βGal (1/2000, MP Biomedicals, Santa Ana, CA, USA; #559761), goat anti-βGal (1/1,000, Biogenesis Ltd., Poole, England, UK; #4600-1409), rabbit anti-Runx1 (1/300, Abcam Inc, Toronto, ON, Canada; #ab92336), rabbit anti-FoxP1 (1/30,000, Abcam; #ab16645), rabbit anti-Pax6 (1/500, Covance/BioLegend, San Diego, CA, USA; # PRB-278P), rabbit anti-CGRP (1/20,000, Peninsula Labs LLC, San Carlos, CA, USA; #T-4032), goat anti-CGRP (1/1,000, Abcam; #ab36001), rabbit anti-PV (1/5,000, Swant, Bellinzona, Switzerland; #PV-28), goat anti-PV (1/5,000, Swant; #PVG-214), rabbit anti-Calbindin (1/1,000, Millipore, Temecula, CA, USA; #AB1778), mouse anti Calbindin (1/500, Abcam; #ab9481); rabbit anti-calretinin (1/500, Millipore; #AB5054), mouse anti-calretinin (1/500; Milipore; #MAB1568) rabbit anti-Phox2b (1/700, Theriault et al. 2004), mouse anti-Isl1 (1/10; clone 39.4D5), mouse anti-Hb9 (1/10; clone 81.5C10) (Developmental Studies Hybridoma Bank, Iowa City, IA, USA), mouse anti-Ki67 (1/200, BD Biosciences, San Jose, CA, USA; #556003), goat anti-ChAT (1/100, Millipore; #AB144P), guinea pig anti-SCIP (1/3000) (Dasen et al. 2008; Philippidou et al. 2012).

Sections were then rinsed in blocking solution, followed by incubation with the appropriate secondary antibodies for 1 h at room temperature. Secondary antibodies against primary reagents raised in various species were conjugated to Alexa Fluor 555 or Alexa Fuor 488 (1/500, Invitrogen). Sections were then rinsed twice with blocking solution and several times with PBS, counterstained with Hoechst 33258 (1/5000, Sigma-Aldrich) for 5 min, rinsed twice with PBS, mounted with Fluoromount- G (Southern Biotech, Birmingham, AL, USA), and examined by fluorescence microscopy. Images were acquired using either a Digital Video Camera mounted on a Zeiss Axioskop 2 microscope or a Retiga EXi Camera (Qimaging, Surrey, BC, Canada) on a Zeiss Axioscope Imager.M1 microscope. Images were digitally assigned to the appropriate red, green or blue channels using Northern Eclipse image acquisition software (Empix Imaging, Inc., Mississauga, ON, Canada).

Image analysis

The number of Hb9/Isl1-positive 12N MNs expressing specific proteins in Tau^{Runx1} and Tau^{Runx1};$Hb9^{Cre}$ littermates were counted every fourth coronal sections of 14 µm each derived from at least three different embryos for each genotype (at least 10 sections per genotype). Acquired images were analyzed using ImageJ software (National Institutes of Health, Bethesda, MD, USA) by counting immune-labeled cells in 12N. The total number of MNs stained for specific markers was then calculated.

Statistical analysis

Statistical comparisons were made using two-tailed Student's t test. All statistical tests were performed with Microsoft Excel software (Microsoft Canada, Mississauga, ON, Canada). Significance level was set at p=0.05. Where applicable, p vales are indicated in the appropriate figures.

Chapter 4: Results

[4.1] Molecular characterization of ventral half of mouse hypoglossal nucleus

Prior to my arrival to the lab, Dr. Xin Chen showed that specific groups of caudal 12N MNs can be distinguished by the expression, or lack, of specific transcription factors, neurotransmitters, and calcium binding proteins (Chen et al., 2015). These findings suggested that dorsomedial 12N MNs innervating intrinsic retrusors express transcription factor FoxP1 but not Runx1, whereas the opposite situation exists in ventromedial 12N MNs innervating intrinsic protrusors. Dr. Chen further characterized dorsomedial FoxP1+ 12N MNs based on their expression of neurotransmitter CGRP and calcium-binding protein PV. Based on these observations, the first aim of this Thesis work was to further identify other molecules that are preferentially expressed in specific regions of the 12N.

[4.1.1] Calbindin D-28k is expressed in ventrolateral 12N compartment

Based on the demonstration that PV and calretinin have restricted expression patterns in the developing 12N (Chen et al., 2015), we characterized the expression of another calcium-binding protein, Calbindin D-28k (Calbindin), in this nucleus. At rostral 12N levels, Calbindin was robustly expressed in dorsal 12N compartments where neither Runx1 nor PV is significantly expressed (Fig. 6a). At caudal levels, Calbindin was expressed in ventrolateral 12N MNs located lateral to Runx1$^+$ ventromedial 12N MNs (Fig. 6a). These Calbindin-expressing MNs co-expressed CGRP, showing that ventrolateral MNs that were previously characterized as CGRP$^+$ are also Calbindin$^+$ (Fig. 6b). Presumably, lack of PV, Calretinin, and FoxP1 expression in ventral 12N also suggests that expression of Calbindin does not overlap with PV, Calretinin, and FoxP1. These observations suggest that distinct calcium-buffering capacities distinguish Runx1-expressing 12N MNs from other, anatomically separate, groups of 12N MNs during

embryonic development. Taken together with previous studies (Chen et al., 2015), these observations provide evidence that the combinatorial expression of Runx1, FoxP1, CGRP, PV and Calbindin defines separate groups of MNs located in at least three separate anatomical regions in the developing mouse 12N. Specifically, ventromedial Runx1^{+} MNs do not express FoxP1 and do not appear to rely on calcium-binding proteins PV, Calretinin, and Calbindin for calcium-buffering capacity. Dorsomedial FoxP1^{+} 12N MNs do not express Runx1 and unlike Runx1^{+} ventromedial neighbors, express calcium-buffering protein PV and neurotransmitter CGRP. Lastly, ventrolateral 12N MNs are characterized by their co-expression of calcium-binding protein Calbindin and neurotransmitter CGRP and by the lack of Runx1, FoxP1, PV, and Calretinin expression.

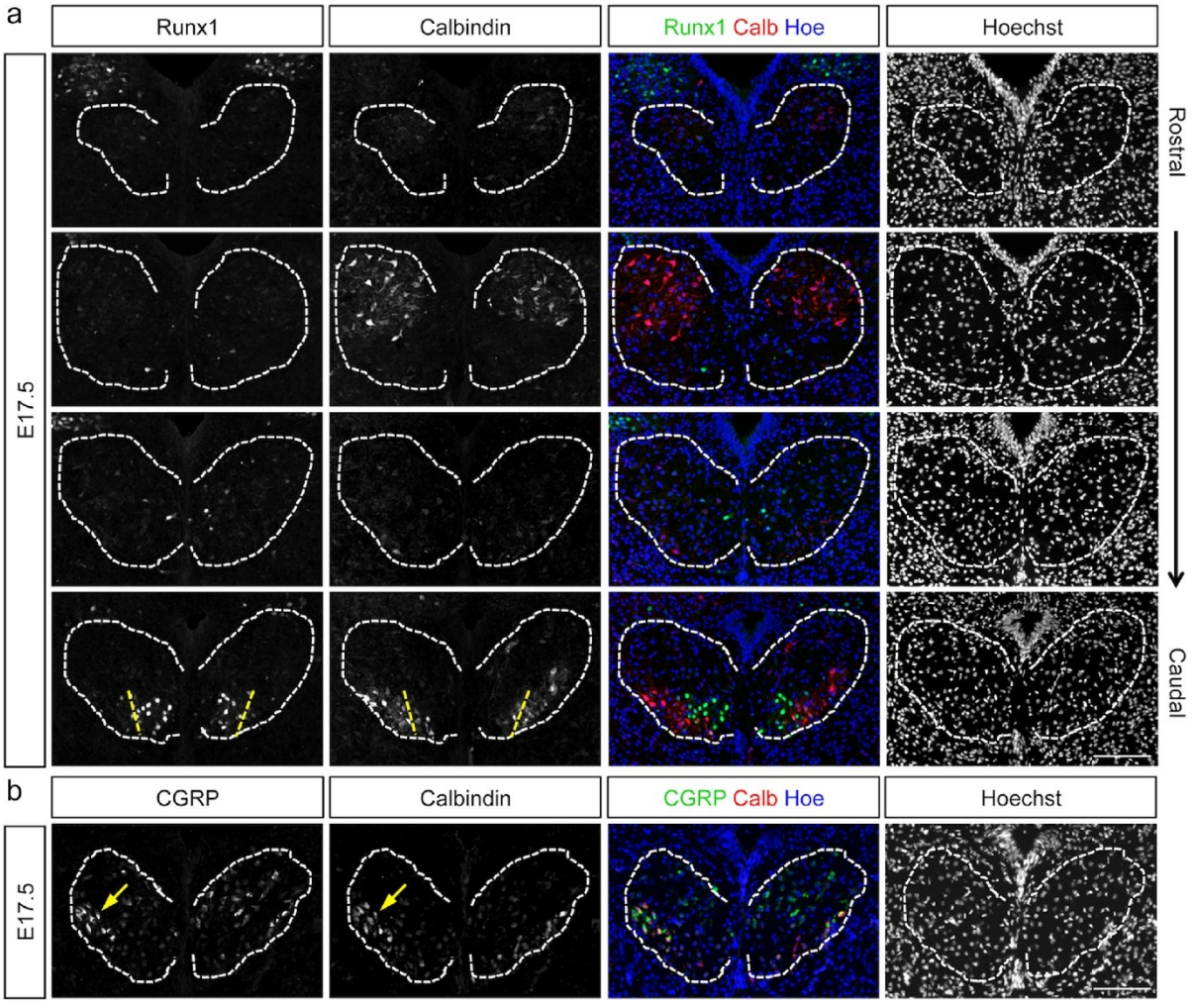

Figure 6. Expression of Runx1, Calbindin and CGRP in mouse embryo hypoglossal nucleus. a. Representative double-labeling immunofluorescence analysis of Runx1 and Calbindin expression in serial coronal sections through 12N of E17.5 embryos. Dotted curved white lines roughly demarcate the perimeter of 12N. Dotted straight yellow lines in bottom panels roughly demarcate the lateral boundary of the ventral Runx1 expression domain in 12N. Scale bar 100 lm. **b.** Representative double-labeling immunofluorescence analysis of CGRP and Calbindin expression in coronal sections through 12N of E17.5 embryos. Dotted curved white lines roughly demarcate the perimeter of 12N. Arrows point to group of double-labeled cells in ventrolateral region. Scale bar 100 μm.

[4.1.2] SCIP expression is correlated with ventral 12N somatotopic organization

Transcription factor SCIP is expressed in selected spinal cord MN populations in mouse and chick embryos, and SCIP and Runx1 mark non-overlapping MN populations in the avian brachial spinal cord (Dasen et al., 2005; Machado et al., 2014; Philippidou et al., 2012). In contrast to the dorsal expression of FoxP1 in 12N, SCIP was expressed preferentially in ventral 12N (Fig. 7a–d, Fig. 8). In this region, SCIP expression appeared to precede that of Runx1 because it was already robustly detected at E13.5 (Fig. 8a), when Runx1 expression in 12N is still sparse (Chen et al., 2015). At both E14.5 and E17.5, SCIP immunoreactivity marked a broad population of ventral 12N MNs that included both a ventromedial Runx1^{+} group and a ventrolateral Runx1^{-} population (Fig. 7a–d, Fig. 8b). Similar to the situation observed when comparing Runx1 and FoxP1, little or no overlap of SCIP and FoxP1 was observed in the ventromedial domain (Fig. 7e–h, Fig. 8c). SCIP immunoreactivity overlapped with Calbindin expression in the ventrolateral region, but not ventromedially (Fig. 9). These results suggest that MNs expressing SCIP alone, or SCIP and Runx1 in combination, define two separate groups of 12N MNs in the lateral or medial part of ventral 12N.

Taken together, these findings provide evidence suggesting that the combinatorial expression of Runx1, SCIP and FoxP1, together with the expression of CGRP, Calbindin and PV, defines at least three separate MN groups in the caudal half of 12N: (1) ventrolateral ($SCIP^+/Runx1^-/FoxP1^-/CGRP^+/Calbindin^+/PV^-$), (2) ventromedial ($SCIP^+/Runx1^+/FoxP1^-/CGRP^-/Calbindin^-/PV^-$) and (3) dorsomedial ($FoxP1^+/Runx1^-/SCIP^-/PV^+/CGRP^+/Calbindin^-$) (summarized in Fig. 10) (Chen et al., 2015). These findings raise the question of what roles such spatially regulated genes might play in the establishment of 12N MN topology. Considering that transcription factors play pivotal roles during development by directly regulating gene expression, we next examined the possible roles of a particular transcription factor, Runx1, in the establishment of 12N somatotopic map development.

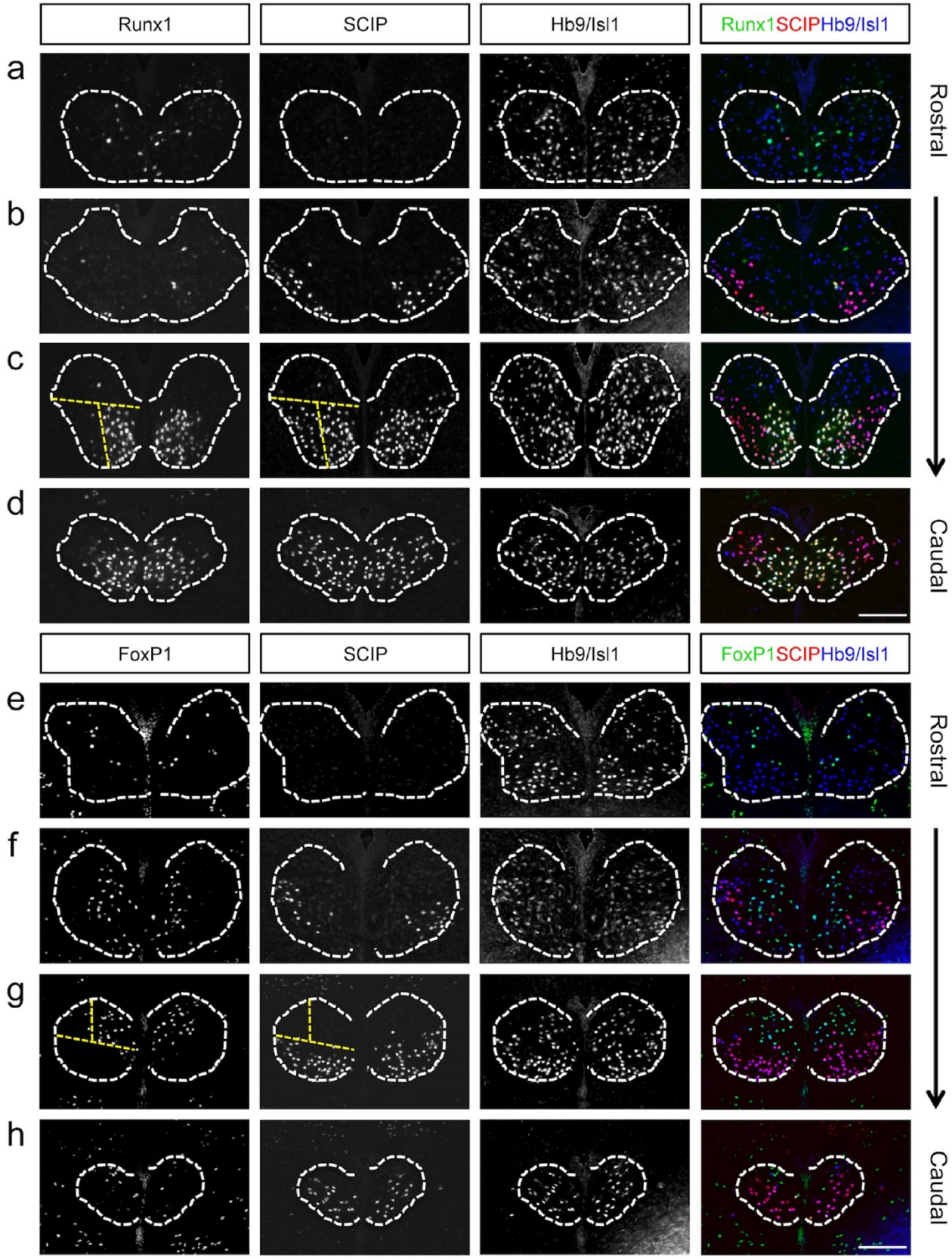
Runx1
SCIP
Hb9/Isl1
Runx1SCIPHb9/Isl1
a
b
c
d
Rostral
Caudal
FoxP1
SCIP
Hb9/Isl1
FoxP1SCIPHb9/Isl1
e
f
g
h
Rostral
Caudal

Figure 7. Combinatorial expression of Runx1, SCIP and FoxP1 defines separate hypoglossal motor neuron groups during embryonic development. **a–h** Triple-labeling immunofluorescence analysis of Runx1, SCIP and Hb9/Isl1 (**a–d**) or FoxP1, SCIP and Hb9/Isl1 (**e-h**) in representative serial coronal sections through 12N of E17.5 mouse embryos. Dotted curved white lines roughly demarcate the perimeter of 12N. Dotted straight yellow lines in (**c**) roughly demarcate the dorsal boundary of SCIP and Runx1 expression and the lateral boundary of Runx1 expression in 12N. Dotted straight yellow lines in (**g**) roughly demarcate the lateral and ventral boundaries of the 12N FoxP1 expression domain. Scale bars 100 μm.

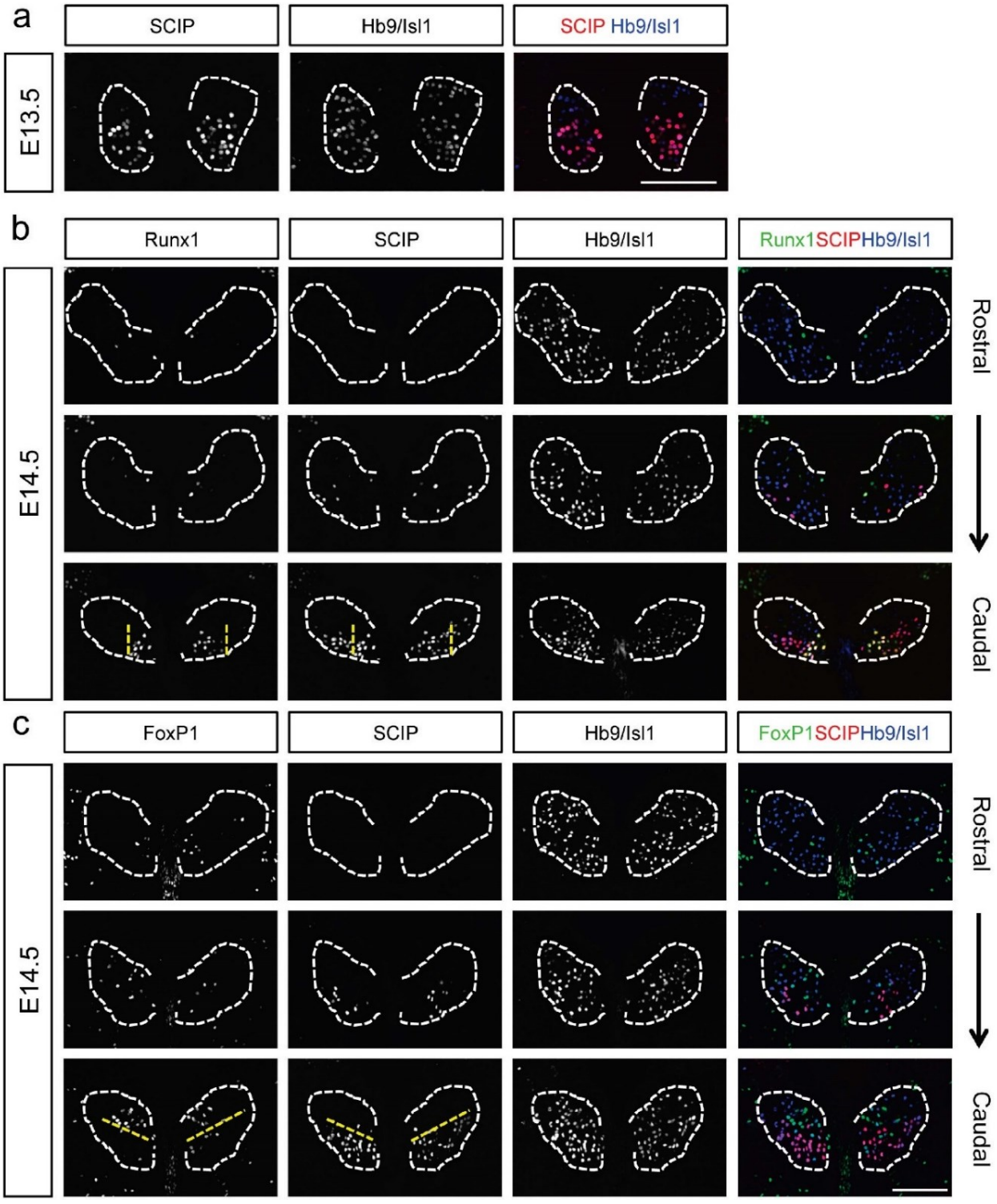
a
SCIP
Hb9/Isl1
SCIP Hb9/Isl1
E13.5
b
Runx1
SCIP
Hb9/Isl1
Runx1SCIPHb9/Isl1
E14.5
Rostral
Caudal
c
FoxP1
SCIP
Hb9/Isl1
FoxP1SCIPHb9/Isl1
E14.5
Rostral
Caudal

Figure. 8. Expression of SCIP, Runx1 and FoxP1 in mouse embryo hypoglossal nucleus. a Representative double-labeling immunofluorescence analysis of SCIP and Hb9/Isl1 expression in coronal sections through 12N of E13.5 embryos. Dotted curved white lines roughly demarcate the perimeter of 12N. Scale bar, 100 μm. **b** Representative triple-labeling immunofluorescence analysis of Runx1, SCIP and Hb9/Isl1 expression in serial coronal sections through 12N of E14.5 embryos. Dotted curved white lines roughly demarcate the perimeter of 12N. Dotted straight yellow lines in bottom panels roughly demarcate the lateral boundary of Runx1 expression domain in 12N. **c** Representative triple-labeling immunofluorescence analysis of FoxP1, SCIP and Hb9/Isl1 expression in serial coronal sections through 12N of E14.5 embryos. Dotted curved white lines roughly demarcate the perimeter of 12N. Dotted straight yellow lines in bottom panels roughly demarcate the dorsal boundary of SCIP expression in 12N. Scale bar, 100 μm.

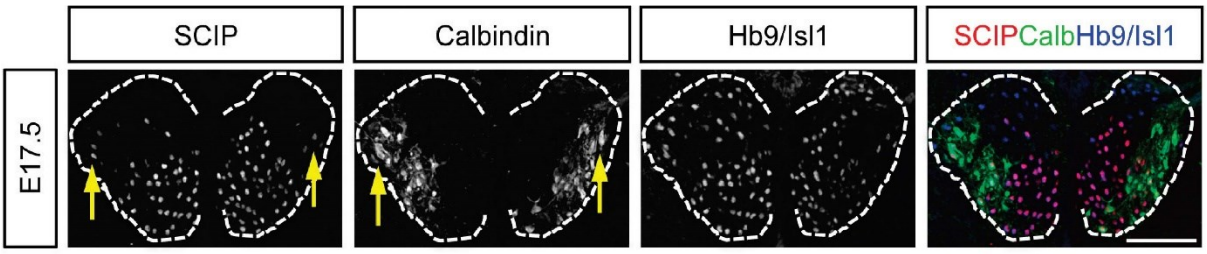

Figure 9. Expression of SCIP and Calbindin in mouse embryo hypoglossal nucleus. Representative double-labeling immunofluorescence analysis of SCIP and Calbindin expression in 12N of E17.5 embryos. Dotted curved white lines roughly demarcate the perimeter of 12N. Arrows point to examples of double-labeled cells in ventrolateral 12N region. Scale bar, 100 μm.

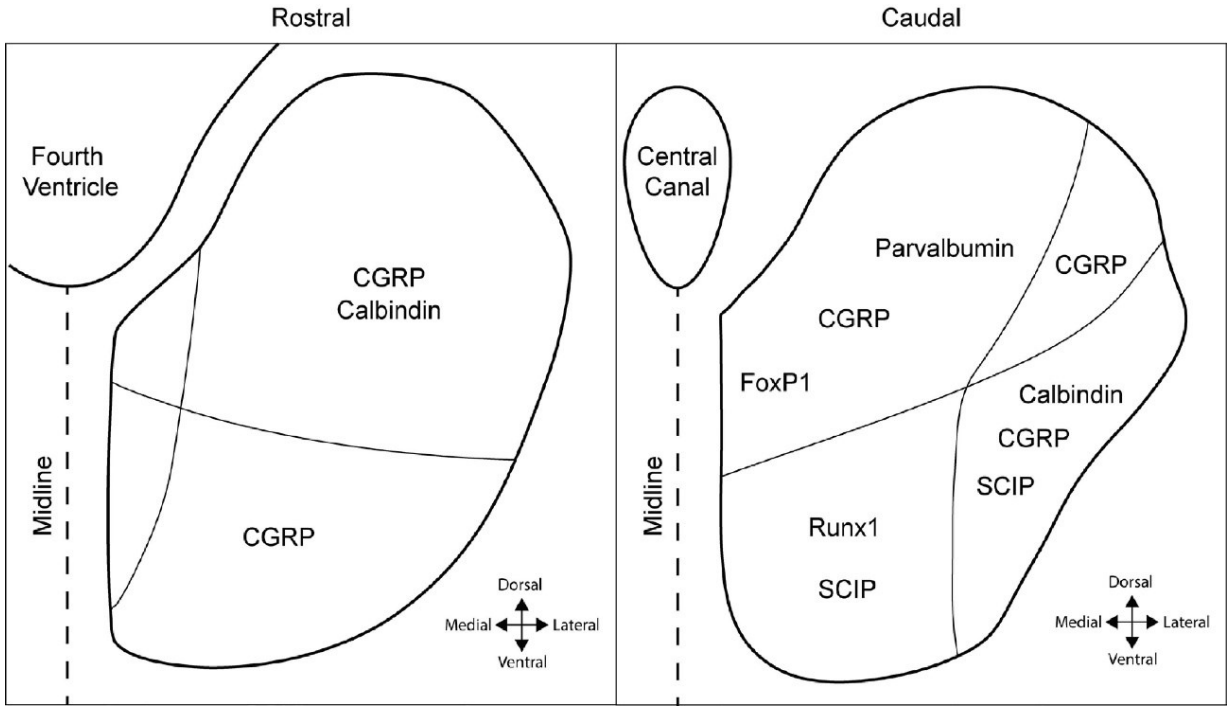

Figure 10. Schematic summary of protein expression patterns in mouse embryo hypoglossal nucleus. Left-hand side: little or no expression of transcription factors Runx1, SCIP and FoxP1 is observed in the rostral part of the mouse 12N during embryonic development. Both CGRP and Calbindin are robustly expressed in the rostral 12N region, where their combinatorial expression defines two broad ventrolateral and dorsolateral 12N domains (delimited by solid lines). Right-hand side: expression of Runx1, SCIP and FoxP1 is mainly observed in the caudal half of 12N, where their combined expression defines dorsomedial, ventromedial, and ventrolateral 12N domains (delimited by solid lines). These MN groups also exhibit specific patterns of CGRP, Calbindin and PV expression. Together, these distinct molecular profiles define separate 12N MN maps along the three body axes.

[4.2] Runx1 is involved in establishment of defined hypoglossal motor neuron maps

To determine whether Runx1 might be important for the formation of 12N MN topographies, we characterized the effect of forcing ectopic Runx1 expression in all developing 12N MNs. Conditional exogenous expression of Runx1 was achieved by utilizing previously described 'Tau-Runx1-LacZ' knock-in mice (Tau^{Runx1} mice) in which a lox-STOP-lox-Runx1-IRES-nLacZ cassette was integrated into the pan-neuronal *Tau* locus to place exogenous Runx1 (and LacZ) expression under the conditional control of the *Tau* promoter (Kramer et al. 2006). Tau^{Runx1} mice were crossed with $Hb9^{Cre}$ mice expressing Cre recombinase under the control of the *Hb9* promoter. As a result of Cre-mediated recombination event, Runx1 and βGal expression was conditionally driven by pan-neuronal promoter *Tau* in somatic MNs. Previous studies have shown that βGal expression in MNs under the control of the *Hb9* (or *Isl1*) promoter has no effect on MN development (Arber et al. 1999; Zhang et al. 2013). The effectiveness of this approach was demonstrated by the expression of Runx1 (together with βGal) in virtually all Hb9-expressing 12N MNs in Tau^{Runx1};$Hb9^{Cre}$ embryos, in contrast to the restricted expression of Runx1 in ventromedial 12N MNs (and absence of βGal) in Tau^{Runx1} control littermates (Fig. 11a,c).

Analysis of coronal sections of 12N ectopically expressing Runx1 (Tau^{Runx1};$Hb9^{Cre}$) showed that exogenous Runx1 was not correlated with any significant change in total MN numbers at both E14.5 and E17.5, compared to control conditions (Fig. 11). However, closer examination of 12N morphology in Tau^{Runx1} and Tau^{Runx1};$Hb9^{Cre}$ littermates revealed an abnormally elongated 12N in embryos conditionally expressing Runx1. Moreover, numerous Hb9-positive MNs could be observed at displaced ventral locations in Tau^{Runx1};$Hb9^{Cre}$ 12N compared to control littermates (Fig. 12a). To better characterize this phenotype, the effects of ectopic Runx1 expression were examined at both rostral and caudal levels of 12N.

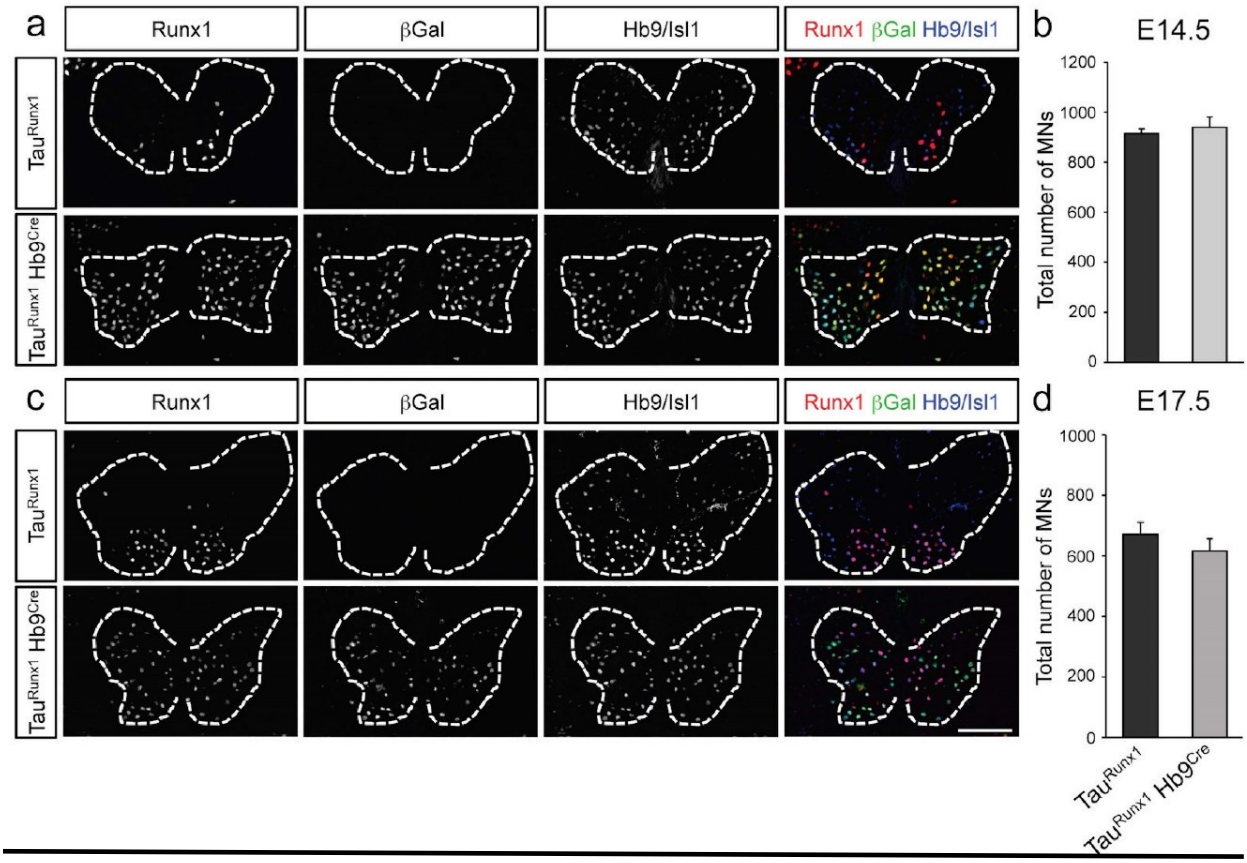

Figure 11. Ectopic Runx1 expression in hypoglossal nucleus at E14.5 and E17.5. **a**, **c** Triple-labeling immunofluorescence analysis of Runx1, βGal and Hb9/Isl1 in representative coronal sections through caudal 12N of E14.5 (**a**) or E17.5 (**c**) *TauRunx1* or *Tau^{Runx1};Hb9^{Cre}* mouse embryos, as indicated. Dotted curved white lines roughly demarcate the perimeter of 12N. Scale bar, 100 μm. **b**, **d** Quantification of total MN numbers in the entire 12N of E14.5 (**b**) or E17.5 (**d**) *Tau^{Runx1}* or *Tau^{Runx1};Hb9^{Cre}* mouse embryos. Results are shown as mean ± SEM (n≥10 sections from each of at least 3 embryos per genotype).

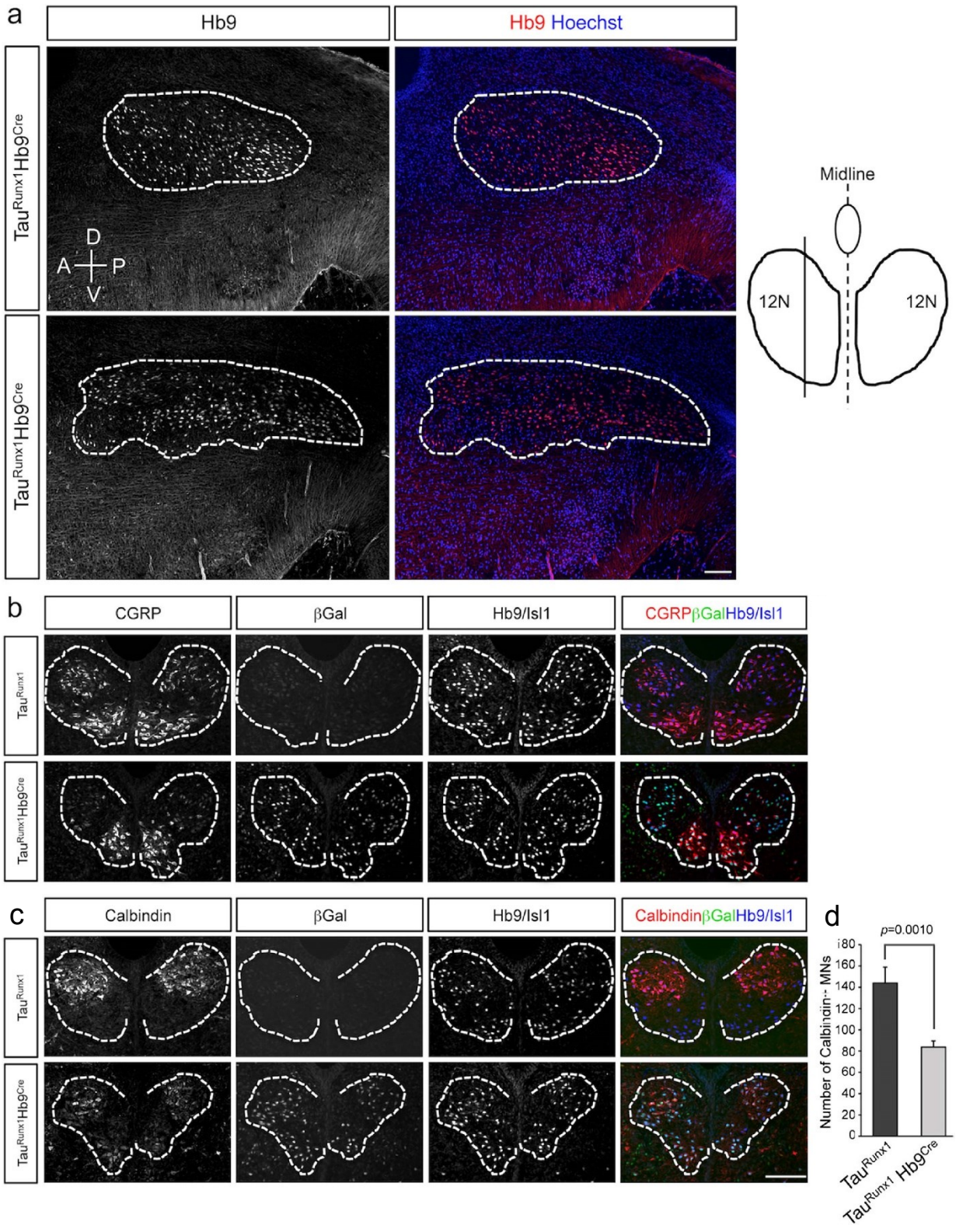
a
Hb9
Hb9 Hoechst
TauRunx1Hb9Cre
TauRunx1Hb9Cre
D
A
P
V
Midline
12N
12N
b
CGRP
βGal
Hb9/Isl1
CGRPβGalHb9/Isl1
TauRunx1
TauRunx1Hb9Cre
c
Calbindin
βGal
Hb9/Isl1
CalbindinβGalHb9/Isl1
TauRunx1
TauRunx1Hb9Cre
d
p=0.0010
Number of Calbindin-- MNs
0
20
40
60
80
100
120
140
160
180
TauRunx1
TauRunx1 Hb9Cre

Figure. 12 Effect of ectopic Runx1 expression in developing hypoglossal nucleus. (**a)** Left-hand side comparison of 12N morphology (visualized through Hb9 expression) in representative sagittal sections through the brainstem of E17.5 Tau^{Runx1} or Tau^{Runx1};$Hb9^{Cre}$ mouse embryos. Dotted curved white lines roughly demarcate the perimeter of 12N. Anterior is to the left and dorsal up. Scale bar 100 lm. Right-hand side: schematic drawing of a coronal view of 12N. Solid line indicates the approximate mediolateral level (roughly 80 lm lateral to the midline) of the sagittal sections shown on the left-hand side of this panel. Dorsal is up. **b** and **c** Triple-labeling immunofluorescence analysis of either CGRP, βGal and Hb9/Isl1 (**b**) or Calbindin, βGal and Hb9/Isl1 (**c**) in representative coronal sections through the rostral 12N of E17.5 Tau^{Runx1} or Tau^{Runx1};$Hb9^{Cre}$ mouse embryos. Dotted curved white lines roughly demarcate the perimeter of 12N. Scale bar 100 μm. (**d**) Quantification of numbers of MNs expressing Calbindin in the rostral half of 12N of E17.5 Tau^{Runx1} or Tau^{Runx1};$Hb9^{Cre}$ mouse embryos. Results are shown as mean ± standard errors of the mean (SEM) (n = 10 sections from each of at least three embryos per genotype; t test)

Rostrally, where little or no endogenous Runx1 is detected, expression of exogenous Runx1 in developing MNs led to a significant decrease in the number of CGRP expressing MNs (Fig. 12b; quantification of these data, which was performed by Dr. Adele Salin Cantegrel, is shown in Chen et al., 2015). A similar decrease in the number of $Calbindin^{+}$ MNs was also observed in the rostral half of 12N of conditional Runx1 transgenic embryos (Fig. 12c,d). These findings suggest that the restricted expression of Runx1 in caudal 12N MNs may be important, at least in part, to delimit the territory containing MNs exhibiting traits characteristics of rostral 12N MNs.

In caudal 12N, expression of Runx1 outside of its physiological ventromedial domain, led to developmental perturbations along both the mediolateral and dorsoventral axes. Along the ventral mediolateral axis, we observed a significant decrease in the number of lateral MNs expressing SCIP and Calbindin, suggestive of a ‘medialization’ of the ventral domain (Fig. 13a–d). Along the medial dorsoventral axis, ectopic Runx1 expression resulted in a considerable decrease in the number of dorsal

cells expressing FoxP1 and PV, suggesting a ‘ventralization’ of the medial domain (Fig. 13e–h). These phenotypes were observed at both E14.5 and E17.5 (Fig. 13, Fig. 14).

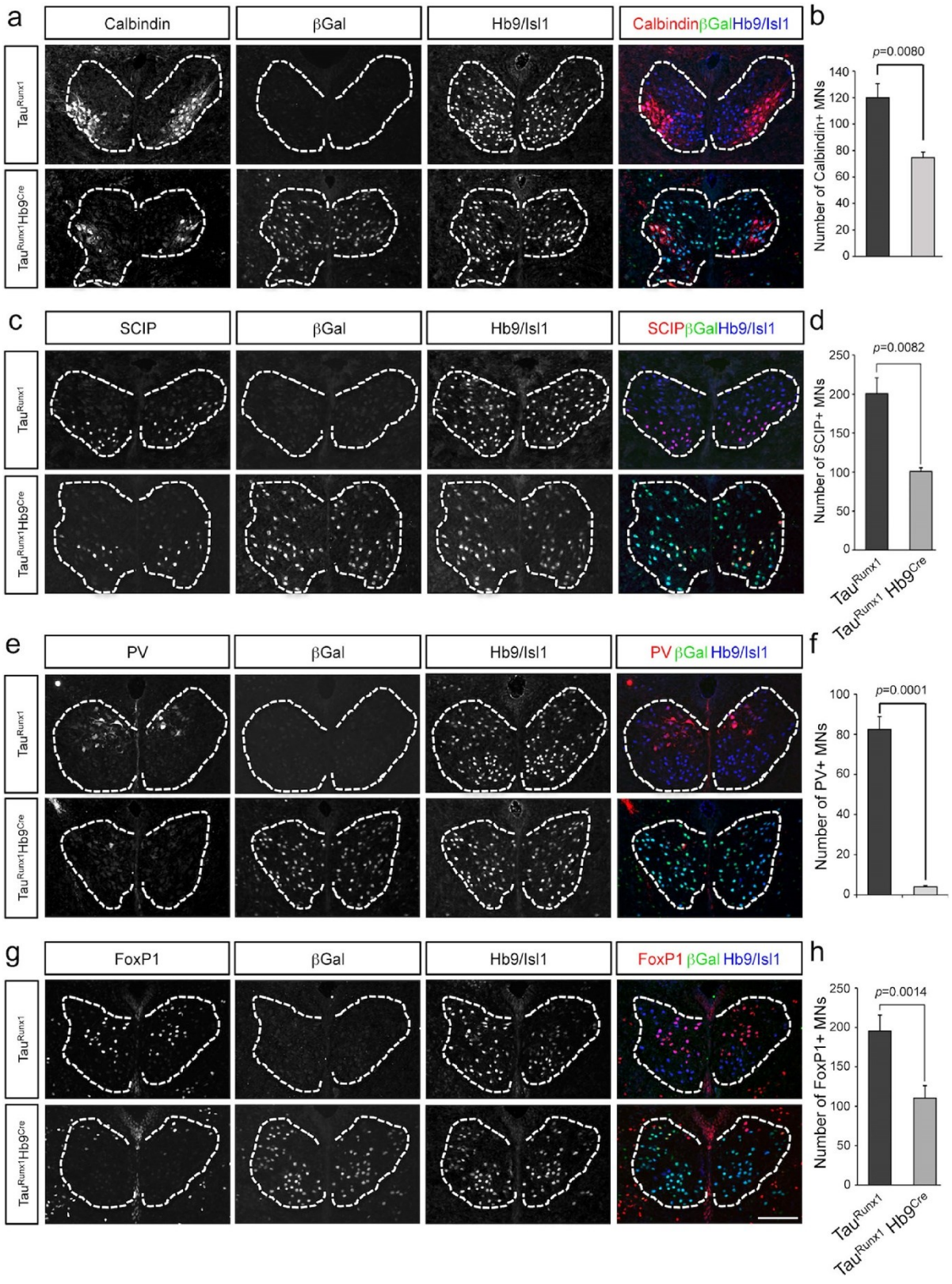

Figure 13. Effect of ectopic Runx1 expression in caudal hypoglossal nucleus during embryonic development. a and c Triple-labeling immunofluorescence analysis of either Calbindin, βGal and Hb9/Isl1 (**a**) or SCIP, βGal and Hb9/Isl1 (**c**) in representative coronal sections through caudal 12N of E17.5 *Tau*^{Runx1} or *Tau*^{Runx1};*Hb9*^{Cre} mouse embryos. Dotted white lines roughly demarcate the perimeter of 12N. b and d Quantification of numbers of MNs expressing either Calbindin (**b**) or SCIP (**d**) in the caudal part of 12N of *Tau*^{Runx1} or *Tau*^{Runx1};*Hb9*^{Cre} mouse embryos. Results are shown as mean ± SEM (n = 10 sections from each of at least 3 embryos per genotype; t test). e and g Triple-labeling immunofluorescence analysis of either PV, βGal and Hb9/Isl1 (**e**) or FoxP1, βGal and Hb9/Isl1 (**g**) in representative coronal sections through 12N of E17.5 *Tau*^{Runx1} or *Tau*^{Runx1}; *Hb9*^{Cre} mouse embryos. Dotted white lines roughly demarcate the perimeter of 12N. Scale bar 100 lm. f and h Quantification of numbers of MNs expressing either PV (**f**) or FoxP1 (**h**) in 12N of E17.5 *Tau*^{Runx1} or *Tau*^{Runx1};*Hb9*^{Cre} mouse embryos. Results are shown as mean ± SEM (n C 10 sections from each of at least three embryos per genotype; t test)

Taken together, these results provide evidence suggesting that Runx1 acts during the establishment of 12N somatotopic organization, at least in part, to prevent the acquisition of ventrolateral and dorsomedial 12N MN molecular profiles in caudal ventromedial MNs, thereby contributing to the specification of 12N MNs innervating intrinsic protrusor muscles (summarized in Fig. 15).

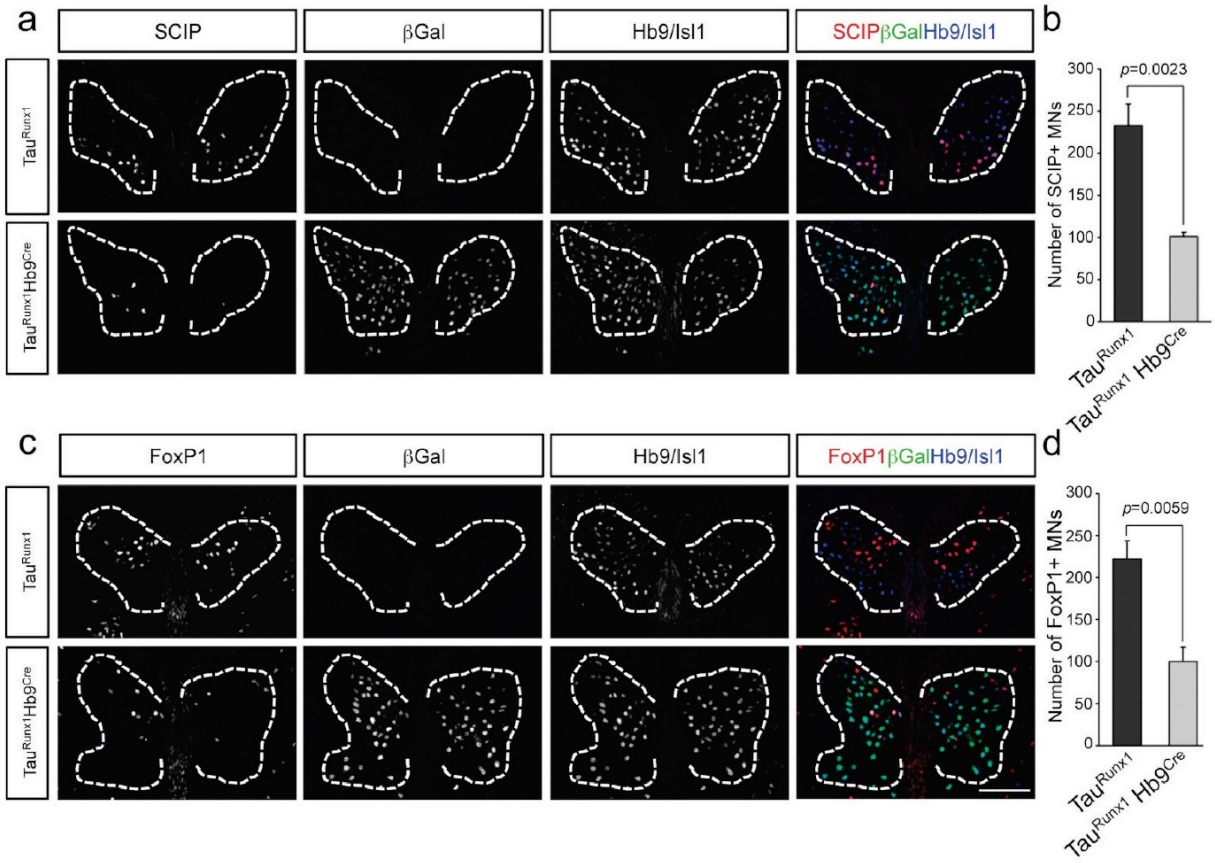

Figure 14. Effect of ectopic Runx1 expression in caudal hypoglossal nucleus at E14.5. **a**, **c** Triple-labeling immunofluorescence analysis of SCIP, βGal and Hb9/Isl1 (**a**) or FoxP1, βGal and Hb9/Isl1 (**c**) in representative coronal sections through 12N of E14.5 *Tau*^{Runx1} or *Tau*^{Runx1}*;Hb9*^{Cre} mouse embryos, as indicated. Dotted white lines roughly demarcate the perimeter of 12N. **b**, **d** Quantification of numbers of MNs expressing SCIP (**b**) or FoxP1 (**d**) in the caudal part of 12N of *Tau*^{Runx1} or *Tau*^{Runx1}*;Hb9*^{Cre} mouse embryos. Results are shown as mean ± SEM (n≥10 sections from each of at least 3 embryos per genotype; *t* test). Scale bar, 100 μm.

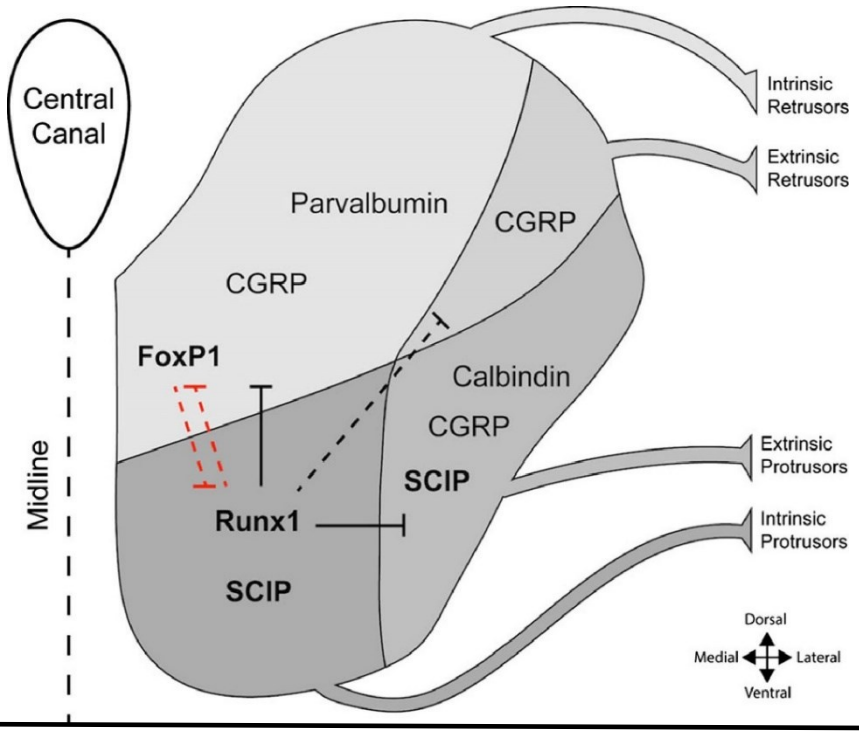

Figure 15. Proposed model of transcriptional regulation of hypoglossal nucleus myotopic organization. Shown is the combinatorial expression of transcription factors Runx1, SCIP and FoxP1 (highlighted in bold face type), calcium-binding proteins PV and Calbindin, and neurotransmitter CGRP in caudal 12N (only one 12N half is depicted). This combinatorial pattern defines four separate MN groups whose position corresponds to 12N anatomical quadrants associated with innervation of different tongue muscle groups. Runx1 is proposed to act in caudal ventromedial 12N MNs to prevent the acquisition of molecular profiles defining dorsomedial (expression of FoxP1, PV and CGRP) and ventrolateral (expression of SCIP, CGRP and Calbindin) 12N MNs (black solid lines). Runx1 may also prevent a dorsolateral 12N MN fate(s) (black dashed line), but testing this possibility further will require the characterization of a specific dorsolateral expression profile. Runx1 and FoxP1 are proposed to cross-repress each other's expression, thereby defining the dorsoventral border of the medial 12N domain (red dashed lines). PV expression may be limited to the dorsomedial quadrant by being under either positive regulation by FoxP1 or negative regulation by Runx1 (or both). Runx1 may directly repress the expression of CGRP and/or Calbindin or may act more generally to promote a specific 12N MN developmental program that is incompatible with expression of these proteins.

Chapter 5: Discussion

The 12N motor circuit is a neural network controlling movements of the tongue. Despite the biological importance of this circuit in control of life-sustaining functions, the development of the 12N circuit is not well-defined. Proper development of 12N MNs is an essential component in the 12N circuit assembly as MNs are the final mediators directly innervating various muscles of the tongue. Much like other MNs found elsewhere, most exemplified in the spinal cord, 12N MNs exhibit somatotopic map development. During somatotopic organization, MN cell bodies organize into developmentally pre-determined coordinates and become specified into different subtypes, determined by specific muscle innervation choices. Hence, the study of somatotopic MN map development is an important and necessary element in understanding how MN subtypes and circuits are established.

Although the '12N anatomical atlas' was recognized decades ago, the molecular characterization of the anatomical compartments, comprising of distinct MN pools innervating specific muscles of the tongue, was yet to be studied. Being aware of the importance of 12N circuit in controlling vital processes such as breathing and swallowing, we addressed the lack of knowledge of molecular mechanisms controlling establishment of distinct 12N MN maps. In this study, we first defined the molecular characteristics that distinguish distinct 12N MN populations along the three body axes. We then demonstrated that the establishment of separate 12N MN molecular maps depends at least in part on the restricted expression of transcription factor Runx1 in ventromedial 12N MNs.

[5.1] From an 'anatomical to a 'molecular' 12N atlas.

During 12N development, cell soma of MNs innervating protrusor muscles of the tongue settle in ventral half of 12N while MNs innervating retrusor muscles settle in the dorsal half. Within the ventral protrusor-innervating 12N compartment, more medially found (ventromedial) MNs innervate intrinsic protrusor muscles while more laterally found (ventrolateral) MNs innervate extrinsic protrusor muscles. In the present study, we attributed previously unrecognized molecular profiles to these anatomically defined MN groups. We have shown that most if not all ventral 12N MNs express the transcription factor SCIP while only the ventromedial MNs innervating intrinsic protrusor muscles (i.e, *verticalis* and *transversus*) co-express SCIP and Runx1. We suggest that Runx1 and SCIP may be involved in establishment of 12N motor circuit important for tongue protrusion. In agreement with this possibility, a recent study utilizing Runx1-deficient mice reported a decrease in 12N MN axon projections to intrinsic *verticalis* and *transversus* tongue muscles compared to control littermates (Yoshikawa et al., 2015). We also suggest that ventrolateral 12N MNs molecularly characterized by the expression of SCIP, calbindin, and CGRP may innervate extrinsic protrusor muscles (i.e, *genioglossus*) (Fig. 15). In accordance, a recent study showed that retrogradely-labelled ventrolateral 12N MNs, from injections into the *genioglossus*, expressed CGRP (Yoshikawa et al., 2015). These combined observations suggest that transcriptional programs regulated by SCIP and Runx1 contribute to the establishment of motor circuits controlling tongue protrusion.

The present investigations have also assigned previously unknown molecular characteristics to another anatomically identified group of MNs located in the dorsomedial quadrant of the caudal half of the nucleus. We have shown that dorsomedial MNs express FoxP1, PV, and CGRP, but neither Runx1 nor SCIP. Together with previous findings that dorsomedial 12N MNs are retrogradely-labelled following tracer injection into intrinsic superior and longitudinal lingual muscles we suggest that dorsomedial 12N MNs expressing FoxP1, PV and CGRP, but not Runx1 or SCIP, may innervate intrinsic retrusor lingual muscles (McClung and Goldberg, 1999).

Considering that FoxP1 plays important roles in cell body settling position and axon targeting in the spinal cord (Dasen et al. 2008; Kania, 2014; Palmesino et al. 2010; Rousso et al. 2008; Stifani, 2014; Surmeli et al. 2011), it is possible that FoxP1 is involved in developmental programs involved in the establishment of 12N circuits responsible for tongue retraction.

[5.2] Biological significance of temporal expression of Runx1, SCIP, and FoxP1 in 12N

The combinatorial expression of three transcription factors, Runx1, SCIP, and FoxP1, molecularly identifies different quadrants of the caudal 12N somatotopic map. The developmental stages when these three transcription factors start being expressed differ. SCIP appears to be the first to be expressed in 12N MNs. Immunoreactivity to SCIP was detected in ventral 12N MNs as early as E13.5 when Runx1 and FoxP1 are scarcely expressed (Fig. 8a). E13.5 is the stage when postmitotic 12N MNs are believed to be acquiring their topologies and establishing connection with target muscles in the tongue. In earlier stages between E11.5 and E12.5, Runx1 expression is detected in neither 12N progenitors nor newly born $Hb9^{+}$ MNs. Instead, Runx1 expression starts being detected at E13.5 and becomes robust by E14.5 (Chen et al., 2015). Similar to Runx1 expression, FoxP1 expression in 12N begins at approximately E14.5 when 12N MNs are innervating the muscles of the tongue. These observations suggest that earlier expression of SCIP at E13.5 may be important for the initial specification of dorsal *vs* ventral 12N MN fates, favoring the latter. In addition, later restricted expression of Runx1 raises the possibility that medial *vs* lateral specification of the ventral 12N occurs after dorsal *vs* ventral specification has occurred. These suggestions are in potential agreement with the morphology of the hypoglossal nerve (12n). The 12n initially exits the hindbrain in one tight bundle, but soon bifurcates into medial and lateral subdivisions. A retrograde labelling study has shown that the dorsal 12N MNs extend axons along the medial subdivision of 12n while ventral 12N MNs extend along the lateral subdivision of the 12n (McClung and Goldberg, 1999). In anterior regions of the tongue, both medial and lateral 12n components further branch

and innervate both intrinsic and extrinsic muscles of the tongue, raising the possibility that innervation choice between intrinsic *vs* extrinsic muscle occurs after the choice between protrusor *vs* retrusor has occurred (McClung and Goldberg, 1999). Taken together, we suggest that SCIP may be important during the establishment of the dorso-ventral axis of 12N and Runx1 may be important for subsequent medio-lateral axis specification in the ventral compartment.

[5.3] 'Ventromedial caudalization' of hypoglossal nucleus by ectopic Runx1 expression

Runx1 expression in 12N continues in its restricted spatial pattern from E14.5 throughout embryogenesis. To characterize the biological significance of this temporally and spatially controlled Runx1 expression pattern, we forced exogenous Runx1 expression in the developing 12N under the control of the *Hb9* promoter, causing both premature and constitutive Runx1 expression in this biological system. Ectopic Runx1 results in an abnormal 12N morphology characterized by a caudal elongation of the nucleus and the presence of ventrally displaced MNs, with a concomitant decrease in the number of MNs expressing rostral, lateral or dorsal 12N MN markers. These results suggest that Runx1 may promote a 'ventromedial caudalization' of 12N by preventing the acquisition of lateral and dorsal MN fates along the mediolateral or dorsoventral axes, respectively.

[5.3.1] 'Ventralization' by ectopic Runx1 expression in caudal 12N

Analysis of molecular alterations in 12N of embryos expressing ectopic Runx1 revealed changes in FoxP1 and SCIP expression that offer some insight into somatotopic MN map formation. One of the consequences of ectopic Runx1 expression in 12N is the decrease in FoxP1 expression in the dorsomedial region. This observation raises the possibility that one of the functions of Runx1 during 12N development is to prevent FoxP1 expression in the ventral sector of the medial region, thereby establishing separate ventromedial ($FoxP1^-$) and dorsomedial ($FoxP1^+$) 12N MN

populations. The dorsoventral separation of Runx1 and FoxP1 expression along the medial domain in turn suggests that the non-overlapping activities of these transcription factors are involved in the formation of separate motor circuits. On the basis of these observations, we propose that both Runx1 and FoxP1 may be involved in the formation of circuits controlling intrinsic tongue muscle innervation, but these factors act separately to define distinct MN groups involved in the control of either intrinsic protrusor ($Runx1^+$ MNs) or intrinsic retrusor ($FoxP1^+$ MNs) muscles (Fig. 9).

Several lines of evidence suggest that Runx1 may repress Foxp1 expression in ventromedial 12N MNs during development. Evidence of RUNX family protein binding to the *FOXP1* locus in human cells is provided by RUNX chromatin immunoprecipitation data available in the ENCODE database. Moreover, Runx binding sites are present within the mouse *Foxp1* locus and Runx1 directly represses the expression of the related *Foxp* family member *Foxp3* in T cells (Bruno et al. 2009; Kitoh et al. 2009; Rudra et al. 2009). Runx1-mediated repression of *Foxp1* expression might explain, at least in part, the loss of dorsomedial PV expression as a result of ectopic Runx1, if FoxP1 was involved in promoting *PV* gene expression. It is also possible that Runx1 itself may act to repress *PV* expression, as suggested by the observation that the Runx family member Runx3 is negatively correlated with PV expression in the mouse PNS (Levanon et al. 2002).

The possible involvement of Runx1 in the negative regulation of *Foxp1* expression in ventromedial 12N MNs might be mirrored by a converse role for FoxP1 in repressing *Runx1* in dorsomedial MNs. This possibility is suggested by the presence of putative FoxP protein binding sites in the mouse *Runx1* locus (Chen et al., 2015) and by ENCODE chromatin immunoprecipitation data showing binding of FOXP proteins to the RUNX1 locus in human cells (Chen et al., 2015). Moreover, previous studies have shown that FoxP1/2/4 antagonize the activity of the Runx family member Runx2 during endochondral ossification (Zhao et al. 2015). Thus, it is conceivable that FoxP1 might act to prevent *Runx1* expression in dorsomedial 12N MNs. Together, these observations suggest that the establishment of non-overlapping $Runx1^+$ and $FoxP1^+$ 12N MN maps may be achieved by transcriptional crosstalk between these transcription factors (Fig. 9). To further test the hypothesis of cross-repression of each other's

expression, chromatin immunoprecipitation studies using dissected 12N samples may could be performed to determine whether Runx1, and/or FoxP1, are localized to the *Foxp1*, and/or *Runx1*, promoter *in vivo*. Based on the results of these studies, transcription assays could be conducted to assess Runx1's ability to directly repress transcription from the *Foxp1* promoter . Reciprocal experiments could be performed to determine whether FoxP1 can repress transcription from the Runx1 promoter. Considering other examples of cross-repressive regulation of transcription factors acting to delineate separate neural cell populations, eg the interactions between Class I and Class II transcriptional factors in the ventral neural tube domains (Briscoe et al., 1999; Briscoe et al., 2000; Jessell, 2000; Vallstedt et al., 2001), it is entirely possible that Runx1 and FoxP1 cross-repress each other's expression to delineate the dorsal-ventral separation of medial 12N.

[5.3.2] 'Medialization' by ectopic Runx1 expression in caudal 12N

Another notable consequence of ectopic Runx1 expression during 12N development is the decrease in the number of $SCIP^+$ cells in the ventral region of the nucleus. SCIP is expressed in ventral 12N MNs both without and with Runx1, suggesting that Runx1 does not directly regulate SCIP expression and that the loss of $SCIP^+$ cells as a result of ectopic Runx1 expression is the consequence of a perturbation of ventrolateral 12N MN developmental programs. This possibility is consistent with the decreased expression of another protein found in ventrolateral 12N MNs, namely Calbindin. It is entirely possible, however, that Runx1 might be able to repress SCIP when exogenously expressed during 12N development at stages preceding its normal onset of expression. This possibility could be due to developmentally regulated changes in the state of the SCIP promoter that would modify its responsiveness to Runx1 or other, Runx1-regulated, transcription factors. Regardless of the precise mechanisms underlying this phenotype, it is important to note that SCIP expression in the ventral 12N is broader than that of Runx1. Moreover, SCIP appears to be already robustly expressed in 12N when Runx1 expression starts. These observations suggest that SCIP may have a more general role in ventral 12N MNs than

Runx1 and that the latter may act to modulate SCIP activity in the ventromedial 12N MN subpopulation, possibly through physical interaction and/or regulation of common genes. In this proposed scenario, both SCIP and Runx1 would be important for the development of ventral 12N MNs controlling protrusor tongue muscles, with ventromedial MNs expressing both SCIP and Runx1 participating in the control of intrinsic protrusor muscles and ventrolateral 12N MNs expressing SCIP alone controlling extrinsic protrusors (Fig. 9).

[5.3.3] Possibility of Runx1-mediated regulation of calcium-binding proteins and implications for ALS

The current study has shown that Runx1 expression does not overlap with three calcium-binding proteins, namely Parvalbumin, Calbinin, and Calretinin in developing 12N MNs. This finding suggests that Runx1 may be either directly or indirectly involved in the negative regulation of the expression of these calcium-binding proteins in the developing ventromedial 12N, thereby contributing to specifying different calcium-buffering capacity for different 12N subpopulations. Although the mechanisms behind this negative correlation remain to be defined, this study has revealed a correlation between an apparent low calcium buffering capacity and Runx1 expression in 12N MNs. This observation acquires a particular interest when considering that MNs with lower expression of calcium-binding proteins are considered to be more susceptible to degeneration in ALS (Leal and Gomes, 2015). Specifically, previous studies have shown that MNs with low expression of calcium-buffering proteins such as Parvalbumin and Calbindin have higher vulnerability to calcium overload (Alexianu et al., 1994; Palecek et al., 1999; Jaiswal, 2013). MNs with low calcium buffering capacity have been postulated to have higher predisposition to intracellular calcium overload commonly detected in degenerating ALS-affected MNs (Siklos et al., 1996; Grosskreutz et al., 2010; Kawamata and Manfredi, 2010). In ALS patients, MNs further downregulate Calretinin and Parvalbumin levels, resulting in calcium overload-mediated degeneration (Hayashi et al., 2013; Leal and Gomes, 2015). Consistently, in the ALS1 mouse model, MNs genetically modified to overexpress calcium-buffering proteins exhibit delayed

symptoms of neurodegeneration (Beers et al., 2001). The possibility of Runx1 involvement in down-regulation of calcium buffering capacity suggested in this study of developing 12N MNs holds implications in modeling ALS-vulnerable MNs *in vitro*. Targeting Runx1 to achieve low calcium-binding protein levels during the derivation of MNs from pluripotent stem/progenitor cells, including induced pluripotent stem cells, might be a strategy to model ALS-vulnerable MNs *in vitro*. Alternatively, derivation of MNs with upregulated levls of calcium-binding proteins might be useful for studying the mechanisms by which calcium-binding proteins serve neuroprotective roles in MNs.

In summary, the present studies suggest that a combinatorial 12N transcription factor atlas, based in part on the complementary expression of Runx1, SCIP and FoxP1, is translated during 12N MN development into separate 12N MN maps correlating with the establishment of distinct motor circuits controlling tongue protrusion or retraction.

Bibliography

Adams, K. L., Rousso, D. L., Umbach, J. A., & Novitch, B. G. (2015). Foxp1-mediated programming of limb-innervating motor neurons from mouse and human embryonic stem cells. Nat Commun, 6, 6778. doi:10.1038/ncomms7778

Alaynick, W. A., Jessell, T. M., & Pfaff, S. L. (2011). SnapShot: spinal cord development. Cell, 146(1), 178-178 e171. doi:10.1016/j.cell.2011.06.038

Aldes, L. D. (1995). Subcompartmental organization of the ventral (protrusor) compartment in the hypoglossal nucleus of the rat. J Comp Neurol, 353(1), 89-108. doi:10.1002/cne.903530109

Alexianu, M. E., Ho, B. K., Mohamed, A. H., La Bella, V., Smith, R. G., & Appel, S. H. (1994). The role of calcium-binding proteins in selective motoneuron vulnerability in amyotrophic lateral sclerosis. Ann Neurol, 36(6), 846-858. doi:10.1002/ana.410360608

Altschuler, S. M., Bao, X., & Miselis, R. R. (1994). Dendritic architecture of hypoglossal motoneurons projecting to extrinsic tongue musculature in the rat. J Comp Neurol, 342(4), 538-550. doi:10.1002/cne.903420404

Alvarez-Medina, R., Cayuso, J., Okubo, T., Takada, S., & Marti, E. (2008). Wnt canonical pathway restricts graded Shh/Gli patterning activity through the regulation of Gli3 expression. Development, 135(2), 237-247. doi:10.1242/dev.012054

Arber, S., Han, B., Mendelsohn, M., Smith, M., Jessell, T. M., & Sockanathan, S. (1999). Requirement for the homeobox gene Hb9 in the consolidation of motor neuron identity. Neuron, 23(4), 659-674.

Badea, T. C., Williams, J., Smallwood, P., Shi, M., Motajo, O., & Nathans, J. (2012). Combinatorial expression of Brn3 transcription factors in somatosensory neurons: genetic and morphologic analysis. J Neurosci, 32(3), 995-1007. doi:10.1523/JNEUROSCI.4755-11.2012

Beers, D. R., Ho, B. K., Siklos, L., Alexianu, M. E., Mosier, D. R., Mohamed, A. H., . . . Appel, S. H. (2001). Parvalbumin overexpression alters immune-mediated increases in intracellular calcium, and delays disease onset in a transgenic model of familial amyotrophic lateral sclerosis. J Neurochem, 79(3), 499-509.

Bermingham, J. R., Jr., Scherer, S. S., O'Connell, S., Arroyo, E., Kalla, K. A., Powell, F. L., & Rosenfeld, M. G. (1996). Tst-1/Oct-6/SCIP regulates a unique step in peripheral myelination and is required for normal respiration. Genes Dev, 10(14), 1751-1762.

Bikeles G (1905) Zur Lokalisation im Rückenmark. DtschZ Nervenheilkd 29(3–4):180–207

Briscoe, J., Pierani, A., Jessell, T. M., & Ericson, J. (2000). A homeodomain protein code specifies progenitor cell identity and neuronal fate in the ventral neural tube. Cell, 101(4), 435-445.

Briscoe, J., Sussel, L., Serup, P., Hartigan-O'Connor, D., Jessell, T. M., Rubenstein, J. L., & Ericson, J. (1999). Homeobox gene Nkx2.2 and specification of neuronal identity by graded Sonic hedgehog signalling. Nature, 398(6728), 622-627. doi:10.1038/19315

Brockington, A., Ning, K., Heath, P. R., Wood, E., Kirby, J., Fusi, N., . . . Shaw, P. J. (2013). Unravelling the enigma of selective vulnerability in neurodegeneration: motor neurons resistant to degeneration in ALS show distinct gene expression characteristics and decreased susceptibility to excitotoxicity. Acta Neuropathol, 125(1), 95-109. doi:10.1007/s00401-012-1058-5

Brunet, J. F., & Pattyn, A. (2002). Phox2 genes - from patterning to connectivity. Curr Opin Genet Dev, 12(4), 435-440.

Bruno, L., Mazzarella, L., Hoogenkamp, M., Hertweck, A., Cobb, B. S., Sauer, S., . . . Merkenschlager, M. (2009). Runx proteins regulate Foxp3 expression. J Exp Med, 206(11), 2329-2337. doi:10.1084/jem.20090226

Chang, I. Y., Kim, S. W., Lee, K. J., & Yoon, S. P. (2008). Calbindin D-28k, parvalbumin and calcitonin gene-related peptide immunoreactivity in the canine spinal cord. Anat Histol Embryol, 37(6), 446-451. doi:10.1111/j.1439-0264.2008.00879.x

Chen, C. L., Broom, D. C., Liu, Y., de Nooij, J. C., Li, Z., Cen, C., . . . Ma, Q. (2006). Runx1 determines nociceptive sensory neuron phenotype and is required for thermal and neuropathic pain. Neuron, 49(3), 365-377. doi:10.1016/j.neuron.2005.10.036

Chen, X., Wang, J. W., Salin-Cantegrel, A., Dali, R., & Stifani, S. (2015). Transcriptional regulation of mouse hypoglossal motor neuron somatotopic map formation. Brain Struct Funct. doi:10.1007/s00429-015-1160-2

Chibuzo, G. A., & Cummings, J. F. (1982). An enzyme tracer study of the organization of the somatic motor center for the innervation of different muscles of the tongue: evidence for two sources. J Comp Neurol, 205(3), 273-281. doi:10.1002/cne.902050307

Choi, B. H. (1981). Radial glia of developing human fetal spinal cord: Golgi, immunohistochemical and electron microscopic study. Brain Res, 227(2), 249-267.

Consortium, E. P. (2012). An integrated encyclopedia of DNA elements in the human genome. Nature, 489(7414), 57-74. doi:10.1038/nature11247

Dasen, J. S., De Camilli, A., Wang, B., Tucker, P. W., & Jessell, T. M. (2008). Hox repertoires for motor neuron diversity and connectivity gated by a single accessory factor, FoxP1. Cell, 134(2), 304-316. doi:10.1016/j.cell.2008.06.019

Dasen, J. S., & Jessell, T. M. (2009). Hox networks and the origins of motor neuron diversity. Curr Top Dev Biol, 88, 169-200. doi:10.1016/S0070-2153(09)88006-X

Dasen, J. S., Liu, J. P., & Jessell, T. M. (2003). Motor neuron columnar fate imposed by sequential phases of Hox-c activity. Nature, 425(6961), 926-933. doi:10.1038/nature02051

Dasen, J. S., Tice, B. C., Brenner-Morton, S., & Jessell, T. M. (2005). A Hox regulatory network establishes motor neuron pool identity and target-muscle connectivity. Cell, 123(3), 477-491. doi:10.1016/j.cell.2005.09.009

Dasen, J. S. (2014). Evolving Hox activity profiles govern diversity in locomotor systems. Dev Cell, 29(2), 171-187. doi:10.1016/j.devcel.2014.03.008

Davis-Dusenbery, B. N., Williams, L. A., Klim, J. R., & Eggan, K. (2014). How to make spinal motor neurons. Development, 141(3), 491-501. doi:10.1242/dev.097410

de Souza, E., Covenas, R., Yi, P., Aguilar, L. A., Lerma, L., Andrade, R., . . . Narvaez, J. A. (2008). Mapping of CGRP in the alpaca (Lama pacos) brainstem. J Chem Neuroanat, 35(4), 346-355. doi:10.1016/j.jchemneu.2008.02.004

Demireva, E. Y., Shapiro, L. S., Jessell, T. M., & Zampieri, N. (2011). Motor neuron position and topographic order imposed by beta- and gamma-catenin activities. Cell, 147(3), 641-652. doi:10.1016/j.cell.2011.09.037

Di Bonito, M., Glover, J. C., & Studer, M. (2013). Hox genes and region-specific sensorimotor circuit formation in the hindbrain and spinal cord. Dev Dyn, 242(12), 1348-1368. doi:10.1002/dvdy.24055

Di Meglio, T., Kratochwil, C. F., Vilain, N., Loche, A., Vitobello, A., Yonehara, K., . . . Rijli, F. M. (2013). Ezh2 orchestrates topographic migration and connectivity of mouse precerebellar neurons. Science, 339(6116), 204-207. doi:10.1126/science.1229326

Du, Z. W., Chen, H., Liu, H., Lu, J., Qian, K., Huang, C. L., . . . Zhang, S. C. (2015). Generation and expansion of highly pure motor neuron progenitors from human pluripotent stem cells. Nat Commun, 6, 6626. doi:10.1038/ncomms7626

Dworkin, S., & Jane, S. M. (2013). Novel mechanisms that pattern and shape the midbrain-hindbrain boundary. Cell Mol Life Sci, 70(18), 3365-3374. doi:10.1007/s00018-012-1240-x

Dykes, I. M., Lanier, J., Eng, S. R., & Turner, E. E. (2010). Brn3a regulates neuronal subtype specification in the trigeminal ganglion by promoting Runx expression during sensory differentiation. Neural Dev, 5, 3. doi:10.1186/1749-8104-5-3

Eccles, R., & Lundberg, A. (1957). Integrative pattern of reflex actions by impulses in large muscle spindle afferents on motoneurones to hip muscles. Experientia, 13(10), 414-415.

Eng, S. R., Dykes, I. M., Lanier, J., Fedtsova, N., & Turner, E. E. (2007). POU-domain factor Brn3a regulates both distinct and common programs of gene expression in the spinal and trigeminal sensory ganglia. Neural Dev, 2, 3. doi:10.1186/1749-8104-2-3

Ericson, J., Briscoe, J., Rashbass, P., van Heyningen, V., & Jessell, T. M. (1997). Graded sonic hedgehog signaling and the specification of cell fate in the ventral neural tube. Cold Spring Harb Symp Quant Biol, 62, 451-466.

Ericson, J., Rashbass, P., Schedl, A., Brenner-Morton, S., Kawakami, A., van Heyningen, V., . . . Briscoe, J. (1997). Pax6 controls progenitor cell identity and neuronal fate in response to graded Shh signaling. Cell, 90(1), 169-180.

Francius, C., & Clotman, F. (2014). Generating spinal motor neuron diversity: a long quest for neuronal identity. Cell Mol Life Sci, 71(5), 813-829. doi:10.1007/s00018-013-1398-x

Fregosi, R. F. (2011). Respiratory related control of hypoglossal motoneurons--knowing what we do not know. Respir Physiol Neurobiol, 179(1), 43-47. doi:10.1016/j.resp.2011.06.023

Gaufo, G. O., Thomas, K. R., & Capecchi, M. R. (2003). Hox3 genes coordinate mechanisms of genetic suppression and activation in the generation of branchial and somatic motoneurons. Development, 130(21), 5191-5201. doi:10.1242/dev.00730

Gaufo, G. O., Wu, S., & Capecchi, M. R. (2004). Contribution of Hox genes to the diversity of the hindbrain sensory system. Development, 131(6), 1259-1266. doi:10.1242/dev.01029

Gilland, E., & Baker, R. (1993). Conservation of neuroepithelial and mesodermal segments in the embryonic vertebrate head. Acta Anat (Basel), 148(2-3), 110-123.

Gomez, L. A., Brusco, A., & Saavedra, J. P. (1990). Immunocytochemical study of S-100 positive glial cells in the brainstem and spinal cord of the rat embryo. Int J Dev Neurosci, 8(1), 55-64.

Gordon, P. H., Mitsumoto, H., & Hays, A. P. (2003). Amyotrophic lateral sclerosis. Sci Aging Knowledge Environ, 2003(35), dn2. doi:10.1126/sageke.2003.35.dn2

Grosskreutz, J., Van Den Bosch, L., & Keller, B. U. (2010). Calcium dysregulation in amyotrophic lateral sclerosis. Cell Calcium, 47(2), 165-174. doi:10.1016/j.ceca.2009.12.002

Grskovic, M., Javaherian, A., Strulovici, B., & Daley, G. Q. (2011). Induced pluripotent stem cells--opportunities for disease modelling and drug discovery. Nat Rev Drug Discov, 10(12), 915-929. doi:10.1038/nrd3577

Guidato, S., Prin, F., & Guthrie, S. (2003). Somatic motoneurone specification in the hindbrain: the influence of somite-derived signals, retinoic acid and Hoxa3. Development, 130(13), 2981-2996.

Guthrie, S. (2007). Patterning and axon guidance of cranial motor neurons. Nat Rev Neurosci, 8(11), 859-871. doi:10.1038/nrn2254

Han, S. S., Williams, L. A., & Eggan, K. C. (2011). Constructing and deconstructing stem cell models of neurological disease. Neuron, 70(4), 626-644. doi:10.1016/j.neuron.2011.05.003

Hayashi, S., Amari, M., & Okamoto, K. (2013). Loss of calretinin- and parvalbumin-immunoreactive axons in anterolateral columns beyond the corticospinal tracts of amyotrophic lateral sclerosis spinal cords. J Neurol Sci, 331(1-2), 61-66. doi:10.1016/j.jns.2013.05.008

Hellstrand, E. (1980). Morphological and histochemical properties of tongue muscles in cat. Acta Physiol Scand, 110(2), 187-198. doi:10.1111/j.1748-1716.1980.tb06650.x

Hultborn, H. (2006). Spinal reflexes, mechanisms and concepts: from Eccles to Lundberg and beyond. Prog Neurobiol, 78(3-5), 215-232. doi:10.1016/j.pneurobio.2006.04.001

Inoue, K., Ito, K., Osato, M., Lee, B., Bae, S. C., & Ito, Y. (2007). The transcription factor Runx3 represses the neurotrophin receptor TrkB during lineage commitment of dorsal root ganglion neurons. J Biol Chem, 282(33), 24175-24184. doi:10.1074/jbc.M703746200

Inoue, K., Ozaki, S., Shiga, T., Ito, K., Masuda, T., Okado, N., . . . Ito, Y. (2002). Runx3 controls the axonal projection of proprioceptive dorsal root ganglion neurons. Nat Neurosci, 5(10), 946-954. doi:10.1038/nn925

Jaiswal, M. K. (2013). Calcium, mitochondria, and the pathogenesis of ALS: the good, the bad, and the ugly. Front Cell Neurosci, 7, 199. doi:10.3389/fncel.2013.00199

Jessell, T. M. (2000). Neuronal specification in the spinal cord: inductive signals and transcriptional codes. Nat Rev Genet, 1(1), 20-29. doi:10.1038/35049541
Jung, H., Mazzoni, E. O., Soshnikova, N., Hanley, O., Venkatesh, B., Duboule, D., &

Kania, A. (2014). Spinal motor neuron migration and the significance of topographic organization in the nervous system. Adv Exp Med Biol, 800, 133-148. doi:10.1007/978-94-007-7687-6_8

Kania, A., & Jessell, T. M. (2003). Topographic motor projections in the limb imposed by LIM homeodomain protein regulation of ephrin-A:EphA interactions. Neuron, 38(4), 581-596.

Kanning, K. C., Kaplan, A., & Henderson, C. E. (2010). Motor neuron diversity in development and disease. Annu Rev Neurosci, 33, 409-440. doi:10.1146/annurev.neuro.051508.135722

Kawamata, H., & Manfredi, G. (2010). Mitochondrial dysfunction and intracellular calcium dysregulation in ALS. Mech Ageing Dev, 131(7-8), 517-526. doi:10.1016/j.mad.2010.05.003

Kitoh, A., Ono, M., Naoe, Y., Ohkura, N., Yamaguchi, T., Yaguchi, H., . . . Sakaguchi, S. (2009). Indispensable role of the Runx1-Cbfbeta transcription complex for in vivo-suppressive function of FoxP3+ regulatory T cells. Immunity, 31(4), 609-620. doi:10.1016/j.immuni.2009.09.003

Kramer, I., Sigrist, M., de Nooij, J. C., Taniuchi, I., Jessell, T. M., & Arber, S. (2006). A role for Runx transcription factor signaling in dorsal root ganglion sensory neuron diversification. Neuron, 49(3), 379-393. doi:10.1016/j.neuron.2006.01.008

Krammer, E. B., Rath, T., & Lischka, M. F. (1979). Somatotopic organization of the hypoglossal nucleus: a HRP study in the rat. Brain Res, 170(3), 533-537.

Lacombe, J., Hanley, O., Jung, H., Philippidou, P., Surmeli, G., Grinstein, J., & Dasen, J. S. (2013). Genetic and functional modularity of Hox activities in the specification of limb-innervating motor neurons. PLoS Genet, 9(1), e1003184. doi:10.1371/journal.pgen.1003184

Lallemend, F., Sterzenbach, U., Hadjab-Lallemend, S., Aquino, J. B., Castelo-Branco, G., Sinha, I., . . . Ernfors, P. (2012). Positional differences of axon growth rates between sensory neurons encoded by Runx3. EMBO J, 31(18), 3718-3729. doi:10.1038/emboj.2012.228

Landmesser, L. (1978). The distribution of motoneurones supplying chick hind limb muscles. J Physiol, 284, 371-389.

Lanier, J., Dykes, I. M., Nissen, S., Eng, S. R., & Turner, E. E. (2009). Brn3a regulates the transition from neurogenesis to terminal differentiation and represses non-neural gene expression in the trigeminal ganglion. Dev Dyn, 238(12), 3065-3079. doi:10.1002/dvdy.22145

Leal, S. S., & Gomes, C. M. (2015). Calcium dysregulation links ALS defective proteins and motor neuron selective vulnerability. Front Cell Neurosci, 9, 225. doi:10.3389/fncel.2015.00225

Lee, S. K., Lee, B., Ruiz, E. C., & Pfaff, S. L. (2005). Olig2 and Ngn2 function in opposition to modulate gene expression in motor neuron progenitor cells. Genes Dev, 19(2), 282-294. doi:10.1101/gad.1257105

Leucht, C., Stigloher, C., Wizenmann, A., Klafke, R., Folchert, A., & Bally-Cuif, L. (2008). MicroRNA-9 directs late organizer activity of the midbrain-hindbrain boundary. Nat Neurosci, 11(6), 641-648. doi:10.1038/nn.2115

Levanon, D., Bettoun, D., Harris-Cerruti, C., Woolf, E., Negreanu, V., Eilam, R., . . . Groner, Y. (2002). The Runx3 transcription factor regulates development and survival of TrkC dorsal root ganglia neurons. EMBO J, 21(13), 3454-3463. doi:10.1093/emboj/cdf370

Lewis, P. R., Flumerfelt, B. A., & Shute, C. C. (1971). The use of cholinesterase techniques to study topographical localization in the hypoglossal nucleus of the rat. J Anat, 110(Pt 2), 203-213.

Li, X., Liu, Z., Qiu, M., & Yang, Z. (2014). Sp8 plays a supplementary role to Pax6 in establishing the pMN/p3 domain boundary in the spinal cord. Development, 141(14), 2875-2884. doi:10.1242/dev.105387

Litingtung, Y., & Chiang, C. (2000). Control of Shh activity and signaling in the neural tube. Dev Dyn, 219(2), 143-154. doi:10.1002/1097-0177(2000)9999:9999<::AID-DVDY1050>3.0.CO;2-Q

Liu, J. P., Laufer, E., & Jessell, T. M. (2001). Assigning the positional identity of spinal motor neurons: rostrocaudal patterning of Hox-c expression by FGFs, Gdf11, and retinoids. Neuron, 32(6), 997-1012.

Lou, S., Duan, B., Vong, L., Lowell, B. B., & Ma, Q. (2013). Runx1 controls terminal morphology and mechanosensitivity of VGLUT3-expressing C-mechanoreceptors. J Neurosci, 33(3), 870-882. doi:10.1523/JNEUROSCI.3942-12.2013

Lou, S., Pan, X., Huang, T., Duan, B., Yang, F. C., Yang, J., . . . Ma, Q. (2015). Incoherent feed-forward regulatory loops control segregation of C-mechanoreceptors, nociceptors, and pruriceptors. J Neurosci, 35(13), 5317-5329. doi:10.1523/JNEUROSCI.0122-15.2015

Lowe, A. A. (1980). The neural regulation of tongue movements. Prog Neurobiol, 15(4), 295-344.

Lowe, A. A. (1984). Tongue movements--brainstem mechanisms and clinical postulates. Brain Behav Evol, 25(2-3), 128-137.

Lu, Q. R., Sun, T., Zhu, Z., Ma, N., Garcia, M., Stiles, C. D., & Rowitch, D. H. (2002). Common developmental requirement for Olig function indicates a motor neuron/oligodendrocyte connection. Cell, 109(1), 75-86.

Machado, C. B., Kanning, K. C., Kreis, P., Stevenson, D., Crossley, M., Nowak, M., . . . Lieberam, I. (2014). Reconstruction of phrenic neuron identity in embryonic stem cell-derived motor neurons. Development, 141(4), 784-794. doi:10.1242/dev.097188

Maden, M. (2007). Retinoic acid in the development, regeneration and maintenance of the nervous system. Nat Rev Neurosci, 8(10), 755-765. doi:10.1038/nrn2212

Malatesta, P., Hartfuss, E., & Gotz, M. (2000). Isolation of radial glial cells by fluorescent-activated cell sorting reveals a neuronal lineage. Development, 127(24), 5253-5263.

Manley, N. R., & Capecchi, M. R. (1997). Hox group 3 paralogous genes act synergistically in the formation of somitic and neural crest-derived structures. Dev Biol, 192(2), 274-288. doi:10.1006/dbio.1997.8765

Mark, M., Lufkin, T., Vonesch, J. L., Ruberte, E., Olivo, J. C., Dolle, P., . . . Chambon, P. (1993). Two rhombomeres are altered in Hoxa-1 mutant mice. Development, 119(2), 319-338.

McClung, J. R., & Goldberg, S. J. (1999). Organization of motoneurons in the dorsal hypoglossal nucleus that innervate the retrusor muscles of the tongue in the rat. Anat Rec, 254(2), 222-230.

McClung, J. R., & Goldberg, S. J. (2000). Functional anatomy of the hypoglossal innervated muscles of the rat tongue: a model for elongation and protrusion of the mammalian tongue. Anat Rec, 260(4), 378-386.

McGinnis, W., & Krumlauf, R. (1992). Homeobox genes and axial patterning. Cell, 68(2), 283-302.

Mehler, M. F., Mabie, P. C., Zhang, D., & Kessler, J. A. (1997). Bone morphogenetic proteins in the nervous system. Trends Neurosci, 20(7), 309-317.

Moqrich, A. (2014). Peripheral pain-sensing neurons: from molecular diversity to functional specialization. Cell Rep, 6(2), 245-246. doi:10.1016/j.celrep.2014.01.018

Mosier, K., & Bereznaya, I. (2001). Parallel cortical networks for volitional control of swallowing in humans. Exp Brain Res, 140(3), 280-289.

Murthy, M., Bocking, S., Verginelli, F., & Stifani, S. (2014). Transcription factor Runx1 inhibits proliferation and promotes developmental maturation in a selected population of inner olfactory nerve layer olfactory ensheathing cells. Gene, 540(2), 191-200. doi:10.1016/j.gene.2014.02.038

Nakamura, S., Senzaki, K., Yoshikawa, M., Nishimura, M., Inoue, K., Ito, Y., . . . Shiga, T. (2008). Dynamic regulation of the expression of neurotrophin receptors by Runx3. Development, 135(9), 1703-1711. doi:10.1242/dev.015248

Nordstrom, U., Maier, E., Jessell, T. M., & Edlund, T. (2006). An early role for WNT signaling in specifying neural patterns of Cdx and Hox gene expression and motor neuron subtype identity. PLoS Biol, 4(8), e252. doi:10.1371/journal.pbio.0040252

North, T., Gu, T. L., Stacy, T., Wang, Q., Howard, L., Binder, M., . . . Speck, N. A. (1999). Cbfa2 is required for the formation of intra-aortic hematopoietic clusters. Development, 126(11), 2563-2575.

Novitch, B. G., Chen, A. I., & Jessell, T. M. (2001). Coordinate regulation of motor neuron subtype identity and pan-neuronal properties by the bHLH repressor Olig2. Neuron, 31(5), 773-789.

Odutola, A. B. (1976). Cell grouping and Golgi architecture of the hypoglossal nucleus of the rat. Exp Neurol, 52(3), 356-371.

Osumi, N., Hirota, A., Ohuchi, H., Nakafuku, M., Iimura, T., Kuratani, S., . . . Eto, K. (1997). Pax-6 is involved in the specification of hindbrain motor neuron subtype. Development, 124(15), 2961-2972.

Palecek, J., Lips, M. B., & Keller, B. U. (1999). Calcium dynamics and buffering in motoneurones of the mouse spinal cord. J Physiol, 520 Pt 2, 485-502.

Palmesino, E., Rousso, D. L., Kao, T. J., Klar, A., Laufer, E., Uemura, O., . . . Kania, A. (2010). Foxp1 and lhx1 coordinate motor neuron migration with axon trajectory choice by gating Reelin signalling. PLoS Biol, 8(8), e1000446. doi:10.1371/journal.pbio.1000446

Pattyn, A., Vallstedt, A., Dias, J. M., Sander, M., & Ericson, J. (2003). Complementary roles for Nkx6 and Nkx2 class proteins in the establishment of motoneuron identity in the hindbrain. Development, 130(17), 4149-4159.

Philippidou, P., & Dasen, J. S. (2013). Hox genes: choreographers in neural development, architects of circuit organization. Neuron, 80(1), 12-34. doi:10.1016/j.neuron.2013.09.020

Philippidou, P., Walsh, C. M., Aubin, J., Jeannotte, L., & Dasen, J. S. (2012). Sustained Hox5 gene activity is required for respiratory motor neuron development. Nat Neurosci, 15(12), 1636-1644. doi:10.1038/nn.3242

Prasad, A., & Hollyday, M. (1991). Development and migration of avian sympathetic preganglionic neurons. J Comp Neurol, 307(2), 237-258. doi:10.1002/cne.903070207

Purves, D., and Williams, S. M. (2004). *Neuroscience.* Sunderland, MA: Sinauer Associates.

Ramón y Cajal S (1989) Recollections of my life, 1st MIT Press pbk. edn. MIT Press, Cambridge, MA

Romanes, G. J. (1951). The motor cell columns of the lumbo-sacral spinal cord of the cat. J Comp Neurol, 94(2), 313-363.

Rousso, D. L., Gaber, Z. B., Wellik, D., Morrisey, E. E., & Novitch, B. G. (2008). Coordinated actions of the forkhead protein Foxp1 and Hox proteins in the columnar

organization of spinal motor neurons. Neuron, 59(2), 226-240. doi:10.1016/j.neuron.2008.06.025

Rudra, D., Egawa, T., Chong, M. M., Treuting, P., Littman, D. R., & Rudensky, A. Y. (2009). Runx-CBFbeta complexes control expression of the transcription factor Foxp3 in regulatory T cells. Nat Immunol, 10(11), 1170-1177. doi:10.1038/ni.1795

Sances, S., Bruijn, L. I., Chandran, S., Eggan, K., Ho, R., Klim, J. R., . . . Svendsen, C. N. (2016). Modeling ALS with motor neurons derived from human induced pluripotent stem cells. Nat Neurosci, 16(4), 542-553. doi:10.1038/nn.4273

Sander, M., Sussel, L., Conners, J., Scheel, D., Kalamaras, J., Dela Cruz, F., . . . German, M. (2000). Homeobox gene Nkx6.1 lies downstream of Nkx2.2 in the major pathway of beta-cell formation in the pancreas. Development, 127(24), 5533-5540.

Sawczuk, A., & Mosier, K. M. (2001). Neural control of tongue movement with respect to respiration and swallowing. Crit Rev Oral Biol Med, 12(1), 18-37.

Sharma, K., Leonard, A. E., Lettieri, K., & Pfaff, S. L. (2000). Genetic and epigenetic mechanisms contribute to motor neuron pathfinding. Nature, 406(6795), 515-519. doi:10.1038/35020078

Sharma, K., Sheng, H. Z., Lettieri, K., Li, H., Karavanov, A., Potter, S., . . . Pfaff, S. L. (1998). LIM homeodomain factors Lhx3 and Lhx4 assign subtype identities for motor neurons. Cell, 95(6), 817-828.

Sharma, R., Hicks, S., Berna, C. M., Kennard, C., Talbot, K., & Turner, M. R. (2011). Oculomotor dysfunction in amyotrophic lateral sclerosis: a comprehensive review. Arch Neurol, 68(7), 857-861. doi:10.1001/archneurol.2011.130

Shirasaki, R., & Pfaff, S. L. (2002). Transcriptional codes and the control of neuronal identity. Annu Rev Neurosci, 25, 251-281. doi:10.1146/annurev.neuro.25.112701.142916

Sienkiewicz, W., Dudek, A., Kaleczyc, J., & Chroszcz, A. (2010). Immunohistochemical characterization of neurones in the hypoglossal nucleus of the pig. Anat Histol Embryol, 39(2), 152-159. doi:10.1111/j.1439-0264.2009.00989.x

Siklos, L., Engelhardt, J., Harati, Y., Smith, R. G., Joo, F., & Appel, S. H. (1996). Ultrastructural evidence for altered calcium in motor nerve terminals in amyotropic lateral sclerosis. Ann Neurol, 39(2), 203-216. doi:10.1002/ana.410390210

Smith, J. C., Goldberg, S. J., & Shall, M. S. (2005). Phenotype and contractile properties of mammalian tongue muscles innervated by the hypoglossal nerve. Respir Physiol Neurobiol, 147(2-3), 253-262. doi:10.1016/j.resp.2005.02.016

Sokoloff, A. J., & Deacon, T. W. (1992). Musculotopic organization of the hypoglossal nucleus in the cynomolgus monkey, Macaca fascicularis. J Comp Neurol, 324(1), 81-93. doi:10.1002/cne.903240107

Sonntag, C. F. (1925). The Comparative Anatomy of the Tongues of the Mammalia.—XII. Summary, Classification and Phylogeny. Proceedings of the Zoological Society of London, 95(2), 701-762. doi:10.1111/j.1096-3642.1925.tb01533.x

Stifani, N. (2014). Motor neurons and the generation of spinal motor neuron diversity. Front Cell Neurosci, 8, 293. doi:10.3389/fncel.2014.00293

Stifani, N., Freitas, A. R., Liakhovitskaia, A., Medvinsky, A., Kania, A., & Stifani, S. (2008). Suppression of interneuron programs and maintenance of selected spinal motor neuron fates by the transcription factor AML1/Runx1. Proc Natl Acad Sci U S A, 105(17), 6451-6456. doi:10.1073/pnas.0711299105

Surmeli, G., Akay, T., Ippolito, G. C., Tucker, P. W., & Jessell, T. M. (2011). Patterns of spinal sensory-motor connectivity prescribed by a dorsoventral positional template. Cell, 147(3), 653-665. doi:10.1016/j.cell.2011.10.012

Takeuchi, J. K., Mileikovskaia, M., Koshiba-Takeuchi, K., Heidt, A. B., Mori, A. D., Arruda, E. P., . . . Bruneau, B. G. (2005). Tbx20 dose-dependently regulates transcription factor networks required for mouse heart and motoneuron development. Development, 132(10), 2463-2474. doi:10.1242/dev.01827

Tanabe, Y., William, C., & Jessell, T. M. (1998). Specification of motor neuron identity by the MNR2 homeodomain protein. Cell, 95(1), 67-80.

Thaler, J., Harrison, K., Sharma, K., Lettieri, K., Kehrl, J., & Pfaff, S. L. (1999). Active suppression of interneuron programs within developing motor neurons revealed by analysis of homeodomain factor HB9. Neuron, 23(4), 675-687.

Thaler, J. P., Lee, S. K., Jurata, L. W., Gill, G. N., & Pfaff, S. L. (2002). LIM factor Lhx3 contributes to the specification of motor neuron and interneuron identity through cell-type-specific protein-protein interactions. Cell, 110(2), 237-249.

Theriault, F. M., Roy, P., & Stifani, S. (2004). AML1/Runx1 is important for the development of hindbrain cholinergic branchiovisceral motor neurons and selected cranial sensory neurons. Proc Natl Acad Sci U S A, 101(28), 10343-10348. doi:10.1073/pnas.0400768101

Tosney, K. W., & Landmesser, L. T. (1985). Development of the major pathways for neurite outgrowth in the chick hindlimb. Dev Biol, 109(1), 193-214.

Tossell, K., Andreae, L. C., Cudmore, C., Lang, E., Muthukrishnan, U., Lumsden, A., . . . Irving, C. (2011). Lrrn1 is required for formation of the midbrain-hindbrain boundary and

organiser through regulation of affinity differences between midbrain and hindbrain cells in chick. Dev Biol, 352(2), 341-352. doi:10.1016/j.ydbio.2011.02.002

Tsuchida, T., Ensini, M., Morton, S. B., Baldassare, M., Edlund, T., Jessell, T. M., & Pfaff, S. L. (1994). Topographic organization of embryonic motor neurons defined by expression of LIM homeobox genes. Cell, 79(6), 957-970.

Uemura-Sumi, M., Mizuno, N., Nomura, S., Iwahori, N., Takeuchi, Y., & Matsushima, R. (1981). Topographical representation of the hypoglossal nerve branches and tongue muscles in the hypoglossal nucleus of macaque monkeys. Neurosci Lett, 22(1), 31-35.

Uemura-Sumi, M., Mizuno, N., Nomura, S., Iwahori, N., Takeuchi, Y., & Matsushima, R. (1981). Topographical representation of the hypoglossal nerve branches and tongue muscles in the hypoglossal nucleus of macaque monkeys. Neurosci Lett, 22(1), 31-35.

Vallstedt, A., Muhr, J., Pattyn, A., Pierani, A., Mendelsohn, M., Sander, M., . . . Ericson, J. (2001). Different levels of repressor activity assign redundant and specific roles to Nkx6 genes in motor neuron and interneuron specification. Neuron, 31(5), 743-755.

Varela-Echavarria, A., Pfaff, S. L., & Guthrie, S. (1996). Differential expression of LIM homeobox genes among motor neuron subpopulations in the developing chick brain stem. Mol Cell Neurosci, 8(4), 242-257. doi:10.1006/mcne.1996.0061

Watari, N., Kameda, Y., Takeichi, M., & Chisaka, O. (2001). Hoxa3 regulates integration of glossopharyngeal nerve precursor cells. Dev Biol, 240(1), 15-31. doi:10.1006/dbio.2001.0447

Wolfram, V., Southall, T. D., Brand, A. H., & Baines, R. A. (2012). The LIM-homeodomain protein islet dictates motor neuron electrical properties by regulating K(+) channel expression. Neuron, 75(4), 663-674. doi:10.1016/j.neuron.2012.06.015

Yamada, T., Pfaff, S. L., Edlund, T., & Jessell, T. M. (1993). Control of cell pattern in the neural tube: motor neuron induction by diffusible factors from notochord and floor plate. Cell, 73(4), 673-686.

Yamada, T., Placzek, M., Tanaka, H., Dodd, J., & Jessell, T. M. (1991). Control of cell pattern in the developing nervous system: polarizing activity of the floor plate and notochord. Cell, 64(3), 635-647.

Yang, F. C., Tan, T., Huang, T., Christianson, J., Samad, O. A., Liu, Y., . . . Ma, Q. (2013). Genetic control of the segregation of pain-related sensory neurons innervating the cutaneous versus deep tissues. Cell Rep, 5(5), 1353-1364. doi:10.1016/j.celrep.2013.11.005

Yoshikawa, M., Hirabayashi, M., Ito, R., Ozaki, S., Aizawa, S., Masuda, T., . . . Shiga, T. (2015). Contribution of the Runx1 transcription factor to axonal pathfinding and muscle innervation by hypoglossal motoneurons. Dev Neurobiol, 75(11), 1295-1314. doi:10.1002/dneu.22285

Yoshikawa, M., Senzaki, K., Yokomizo, T., Takahashi, S., Ozaki, S., & Shiga, T. (2007). Runx1 selectively regulates cell fate specification and axonal projections of dorsal root ganglion neurons. Dev Biol, 303(2), 663-674. doi:10.1016/j.ydbio.2006.12.007

Zagami, C. J., & Stifani, S. (2010). Molecular characterization of the mouse superior lateral parabrachial nucleus through expression of the transcription factor Runx1. PLoS One, 5(11), e13944. doi:10.1371/journal.pone.0013944

Zhao, H., Zhou, W., Yao, Z., Wan, Y., Cao, J., Zhang, L., . . . Guo, X. (2015). Foxp1/2/4 regulate endochondral ossification as a suppresser complex. Dev Biol, 398(2), 242-254. doi:10.1016/j.ydbio.2014.12.007

Zhang, T., Liu, J., Zhang, J., Thekkethottiyil, E. B., Macatee, T. L., Ismat, F. A., . . . Stoller, J. Z. (2013). Jun is required in Isl1-expressing progenitor cells for cardiovascular development. PLoS One, 8(2), e57032. doi:10.1371/journal.pone.0057032

Zhou, Q., & Anderson, D. J. (2002). The bHLH transcription factors OLIG2 and OLIG1 couple neuronal and glial subtype specification. Cell, 109(1), 61-73.

Zou, M., Li, S., Klein, W. H., & Xiang, M. (2012). Brn3a/Pou4f1 regulates dorsal root ganglion sensory neuron specification and axonal projection into the spinal cord. Dev Biol, 364(2), 114-127. doi:10.1016/j.ydbio.2012.01.021

Zusso, M., Methot, L., Lo, R., Greenhalgh, A. D., David, S., & Stifani, S. (2012). Regulation of postnatal forebrain amoeboid microglial cell proliferation and development by the transcription factor Runx1. J Neurosci, 32(33), 11285-11298. doi:10.1523/JNEUROSCI.6182-11.2012